

UNCLASSIFIED

AD NUMBER

AD888694

LIMITATION CHANGES

TO:

Approved for public release; distribution is unlimited.

FROM:

Distribution authorized to U.S. Gov't. agencies only; Test and Evaluation; OCT 1971. Other requests shall be referred to Air Force Armament Laboratory, Attn: DLGD, Eglin AFB, FL 32542.

AUTHORITY

ADTC ltr, 4 Aug 1976

THIS PAGE IS UNCLASSIFIED

NOV 10 1971

AEDC-TR-71-228 C.2  
AFATL-TR-71-134



# SEPARATION CHARACTERISTICS OF THE LAU-69/A ROCKET LAUNCHER FROM THE F-4C AIRCRAFT AT MACH NUMBERS FROM 0.29 TO 0.78

A. C. Mansfield

ARO, Inc.

October 1971

*This document has been approved for public release  
its distribution is unlimited. JRM  
TAB # 26-24 NOV 1976*

Distribution limited to U. S. Government agencies only;  
this report contains information on test and evaluation  
of military hardware; October 1971; other requests for  
this document must be referred to Air Force Armament  
Laboratory (DLGC), Eglin AFB, Florida 32542.

**PROPULSION WIND TUNNEL FACILITY  
ARNOLD ENGINEERING DEVELOPMENT CENTER  
AIR FORCE SYSTEMS COMMAND  
ARNOLD AIR FORCE STATION, TENNESSEE**

PROPERTY OF U S AIR FORCE  
AEDC LIBRARY  
F40600-72-C-0003

# ***NOTICES***

When U. S. Government drawings specifications, or other data are used for any purpose other than a definitely related Government procurement operation, the Government thereby incurs no responsibility nor any obligation whatsoever, and the fact that the Government may have formulated, furnished, or in any way supplied the said drawings, specifications, or other data, is not to be regarded by implication or otherwise, or in any manner licensing the holder or any other person or corporation, or conveying any rights or permission to manufacture, use, or sell any patented invention that may in any way be related thereto.

Qualified users may obtain copies of this report from the Defense Documentation Center.

References to named commercial products in this report are not to be considered in any sense as an endorsement of the product by the United States Air Force or the Government.

**SEPARATION CHARACTERISTICS OF THE LAU-69/A  
ROCKET LAUNCHER FROM THE F-4C AIRCRAFT AT  
MACH NUMBERS FROM 0.29 TO 0.78**

**A. C. Mansfield  
ARO, Inc.**

Distribution limited to U. S. Government agencies only;  
this report contains information on test and evaluation  
of military hardware; October 1971; other requests for  
this document must be referred to Air Force Armament  
Laboratory (DLGC), Eglin AFB, Florida 32542.

## FOREWORD

The work reported herein was sponsored by the Air Force Armament Laboratory (DLGC/Bob Hume), Armament Development and Test Center, Air Force Systems Command (AFSC), under Program Element 64602F, Project 2592, Task 04.

The test results presented were obtained by ARO, Inc. (a subsidiary of Sverdrup & Parcel and Associates, Inc.), contract operator of the Arnold Engineering Development Center (AEDC), AFSC, Arnold Air Force Station, Tennessee, under Contract F40600-72-C-0003. The test was conducted from August 2 to 8, 1971, under ARO Project No. PC0161. The manuscript was submitted for publication on September 21, 1971.

This technical report has been reviewed and is approved.

George F. Garey  
Lt Colonel, USAF  
AF Representative, PWT  
Directorate of Test

Duncan W. Rabey, Jr.  
Colonel, USAF  
Director of Test

### ABSTRACT

A wind-tunnel test was conducted using 0.05-scale models to study the separation characteristics of the LAU-69/A rocket launcher, both full and empty, from the F-4C aircraft. The separation trajectories were initiated from the right-wing inboard pylon station utilizing the Triple Ejection Rack and from the centerline pylon utilizing the Multiple Ejection Rack. A 370-gal fuel tank was mounted on the outboard pylon. The flight conditions simulated were Mach numbers from 0.29 to 0.78 at an altitude of 5000 ft. For all test conditions, the parent aircraft was in unaccelerated level flight. Also, static stability, axial-force, and trajectory data were obtained for the empty launcher with and without flow through the empty launcher tubes.

## CONTENTS

	<u>Page</u>
ABSTRACT . . . . .	iii
NOMENCLATURE . . . . .	vii
I. INTRODUCTION . . . . .	1
II. APPARATUS . . . . .	
2.1 Test Facility . . . . .	1
2.2 Test Articles . . . . .	2
2.3 Instrumentation . . . . .	2
III. TEST DESCRIPTION . . . . .	
3.1 Test Conditions . . . . .	3
3.2 Trajectory Data Acquisition . . . . .	3
3.3 Corrections . . . . .	4
3.4 Precision of Data . . . . .	4
IV. RESULTS AND DISCUSSION . . . . .	
4.1 General . . . . .	4
4.2 LAU-69/A, Full . . . . .	5
4.3 LAU-69/A, Empty . . . . .	6
4.4 Comparison of Empty Launcher with Tubes Open and Closed . . . . .	6
REFERENCES . . . . .	6

## APPENDIXES

### I. ILLUSTRATIONS

#### Figure

1. Isometric Drawing of a Typical Store Separation Installation and a Block Diagram of the Computer Control Loop . . . . .	9
2. Schematic of the Tunnel Test Section Showing Model Location . . . . .	10
3. Sketch of the F-4 Parent-Aircraft Model . . . . .	11
4. Details and Dimensions of the F-4 Inboard and Centerline Pylon Model . . . . .	12
5. Details and Dimensions of the F-4 370-gal Fuel Tank Model . . . . .	13
6. Details and Dimensions of the TER Model . . . . .	14
7. Details and Dimensions of the MER Model . . . . .	15
8. Details and Dimensions of the LAU-69/A Metric and Dummy Rocket Launcher Models (Full) . . . . .	16
9. Details and Dimensions of the LAU-69/A Rocket Launcher Models (Empty)	
a. Metric Model . . . . .	17
b. Dummy Model . . . . .	18
10. Schematic of TER and MER Store Stations and Orientations . . . . .	19
11. Tunnel Installation Photograph Showing Parent Aircraft, Store, and CTS . . . . .	20

<u>Figure</u>	<u>Page</u>
12. TER and MER Ejector Force Functions	
a. LAU-69/A, Full . . . . .	21
b. LAU-69/A, Empty . . . . .	22
13. Effect of Mach Number on the Separation Characteristics of the LAU-69/A (Full with the Heavy Warhead) from the Inboard TER and Centerline MER	
a. TER, Configuration 1H, MER Forward . . . . .	23
b. TER, Configuration 2H, MER Aft . . . . .	24
c. TER, Configuration 3H, MER Forward . . . . .	25
d. TER, Configuration 4H, MER Forward . . . . .	26
e. TER, Configuration 5H, MER Forward . . . . .	27
f. TER, Configuration 6H, MER Forward . . . . .	28
g. MER, Configuration 7H, MER Aft . . . . .	29
h. MER, Configuration 8H, MER Aft . . . . .	30
i. MER, Configuration 9H, MER Aft . . . . .	31
14. Effects of Mach Number on the Separation Characteristics of the LAU-69/A (Full with the Light Warhead) from the Inboard TER and Centerline MER	
a. TER, Configuration 1L, MER Forward . . . . .	32
b. TER, Configuration 2L, MER Aft . . . . .	33
c. TER, Configuration 3L . . . . .	34
d. TER, Configuration 4L, MER Forward . . . . .	35
e. TER, Configuration 5L, MER Forward . . . . .	36
f. TER, Configuration 6L, MER Aft . . . . .	37
g. MER, Configuration 7L, MER Aft . . . . .	38
h. MER, Configuration 8L, MER Aft . . . . .	39
i. MER, Configuration 9L, MER Aft . . . . .	40
15. Comparison of Trajectories of the Full LAU-69/A from the TER with MER in Forward and Aft Locations	
a. $M_\infty = 0.78$ , Configuration 6L, $\alpha = 0.9$ . . . . .	41
b. $M_\infty = 0.70$ , Configuration 6L, $\alpha = 1.4$ . . . . .	42
c. $M_\infty = 0.70$ , Configuration 3L, $\alpha = 1.4$ . . . . .	43
16. Effect of Mach Number on the Separation Characteristics of the LAU-69/A (Empty) from the Inboard TER and Centerline MER	
a. TER, Configuration 1E, MER Aft . . . . .	44
b. TER, Configuration 2E, MER Aft . . . . .	45
c. TER, Configuration 3E, MER Aft . . . . .	46
d. TER, Configuration 4E, MER Aft . . . . .	47
e. TER, Configuration 5E, MER Aft . . . . .	48
f. TER, Configuration 6E, MER Aft . . . . .	49
g. MER, Configuration 7E, MER Aft . . . . .	50
h. MER, Configuration 8E, MER Aft . . . . .	51
i. MER, Configuration 9E, MER Aft . . . . .	52



<u>Figure</u>	<u>Page</u>
17. Free-Stream Static Stability and Axial-Force Data Comparing Open and Closed Tubes, LAU-69/A, Empty, for $M_\infty = 0.37, 0.62, \text{ and } 0.78$ . . . . .	53
18. Comparisons of Trajectories Obtained with Open and Closed Tubes, LAU-69/A, Empty, Configuration 5E, MER Aft	
a. $M_\infty = 0.62, \alpha = 1.0$ . . . . .	54
b. $M_\infty = 0.78, \alpha = 0.6$ . . . . .	55

## II. TABLES

I. Summary of Test Conditions . . . . .	56
II. Full-Scale Store Parameters Used in Trajectory Calculations . . . . .	57
III. Load Configurations . . . . .	58

## NOMENCLATURE

BL	Aircraft buttock line from plane of symmetry, in., model scale
b	Store reference dimension, 1.308 ft full scale
$C_A$	Store axial-force coefficient, axial force/ $q_\infty S$
$C_m$	Store pitching-moment coefficient, referenced to the store cg, pitching moment/ $q_\infty S b$
$\dot{C}_{m q}$	Store pitch-damping derivative, $dC_m/d(qb/2V_\infty)$
$C_n$	Store yawing-moment coefficient, referenced to the store cg, yawing moment/ $q_\infty S b$
$\dot{C}_{n r}$	Store yaw-damping derivative, $dC_n/d(rb/2V_\infty)$
$C_y$	Store side-force coefficient, side force/ $q_\infty S$
FS	Aircraft fuselage station, in., model scale
$I_{xx}$	Full-scale moment of inertia about the store $X_B$ axis, slug-ft <sup>2</sup>
$I_{yy}$	Full-scale moment of inertia about the store $Y_B$ axis, slug-ft <sup>2</sup>
$I_{zz}$	Full-scale moment of inertia about the store $Z_B$ axis, slug-ft <sup>2</sup>
$M_\infty$	Free-stream Mach number
m	Full-scale store mass, slugs

$p_{\infty}$	Free-stream static pressure, psfa
$q$	Store angular velocity about the $Y_B$ axis, radians/sec
$q_{\infty}$	Free-stream dynamic pressure $0.7 p_{\infty} M_{\infty}^2$ , psf
$r$	Store angular velocity about the $Z_B$ axis, radians/sec
$S$	Store reference area, $1.344 \text{ ft}^2$ , full scale
$t$	Real trajectory time from initiation of trajectory, sec
$V_{\infty}$	Free-stream velocity, ft/sec
$WL$	Aircraft waterline from reference horizontal plane, in., model scale
$X$	Separation distance of the store cg parallel to the flight axis system $X_F$ direction, ft, full scale measured from the prelaunch position
$X_{cg}$	Full-scale cg location, ft, from nose of store
$X_L$	Ejector piston location relative to the store cg, positive forward of store cg, ft, full scale
$Y$	Separation distance of the store cg parallel to the flight axis system $Y_F$ direction, ft, full scale measured from the prelaunch position
$Z$	Separation distance of the store cg parallel to the flight-axis system $Z_F$ direction, ft, full scale measured from the prelaunch position
$\alpha$	Parent-aircraft model angle of attack relative to the free-stream velocity vector, deg
$\theta$	Angle between the store longitudinal axis and its projection in the $X_F$ - $Y_F$ plane, positive when store nose is raised as seen by pilot, deg
$\chi$	Angle between the projection of the store longitudinal axis in the $X_F$ - $Y_F$ plane and the $X_F$ axis, positive when the store nose is to the right as seen by the pilot, deg

## FLIGHT-AXIS SYSTEM COORDINATES

### Directions

$X_F$	Parallel to the free-stream wind vector, positive direction is forward as seen by the pilot
-------	---

- $X_F$  Perpendicular to the  $X_F$  and  $Z_F$  directions, positive direction is to the right as seen by the pilot
- $Z_F$  In the aircraft plane of symmetry, perpendicular to the free-stream wind vector, positive direction is downward

The flight-axis system origin is coincident with the aircraft cg and remains fixed with respect to the parent aircraft during store separation. The  $X_F$ ,  $Y_F$ , and  $Z_F$  coordinate axes do not rotate with respect to the initial flight direction and attitude.

## STORE BODY-AXIS SYSTEM COORDINATES

### Directions

- $X_B$  Parallel to the store longitudinal axis, positive direction is upstream in the prelaunch position
- $Y_B$  Perpendicular to the store longitudinal axis, and parallel to the flight-axis system  $X_F$ - $Y_F$  plane when the store is at zero roll angle, positive direction is to the right looking upstream when the store is at zero yaw and roll angles
- $Z_B$  Perpendicular to both the  $X_B$  and  $Y_B$  axes, positive direction is downward as seen by the pilot when the store is at zero pitch and roll angles.

The store body-axis system origin is coincident with the store cg and moves with the store during separation from the parent airplane. The  $X_B$ ,  $Y_B$ , and  $Z_B$  coordinate axes rotate with the store in pitch, yaw, and roll so that mass moments of inertia about the three axes are not time-varying quantities.

## SECTION I INTRODUCTION.

In the development of the Pave Rock weapon system, it was required that both empty and full configurations of the LAU-69/A rocket launcher be qualified for separation from the F-4C aircraft. One step in qualifying a store for release from an aircraft is the evaluation of the wind-tunnel-generated store separation data. Using a six-degree-of-freedom captive trajectory store separation system (CTS), trajectory trends may be obtained to aid in determination of the store separation envelopes. Therefore, the separation characteristics of the LAU-69/A rocket launcher from the F-4C aircraft were determined using the captive trajectory system in the Aerodynamic Wind Tunnel (4T) of the Propulsion Wind Tunnel Facility (PWT).

The test was conducted using 0.05-scale models of the F-4C parent aircraft and the LAU-69/A full and empty launchers. The separation trajectories were initiated from the Triple Ejection Rack (TER) mounted on the inboard pylon of the right wing and the Multiple Ejection Rack (MER) mounted on the centerline pylon of the aircraft. The 370-gal fuel tank was mounted on the outboard pylon of the right wing. Trajectory data were obtained at Mach numbers from 0.29 to 0.78 using simulated store weights, center-of-gravity locations, and angles of attack corresponding to the specific flight conditions. A constant altitude of 5000 ft was simulated. The ejector forces were time-variant functions provided by Air Force Armament Laboratory.

Some static stability, axial force, and trajectory data were obtained for the empty launchers with a closed flat face as well as with the launcher tubes open to the passage of air flow. These data were obtained in order to determine if any significant differences could be observed.

## SECTION II APPARATUS

### 2.1 TEST FACILITY

The Aerodynamic Wind Tunnel (4T) is a closed-loop, continuous flow, variable density tunnel in which the Mach number can be varied from 0.1 to 1.3. At all Mach numbers, the stagnation pressure can be varied from 300 to 3700 psfa. The test section is 4 ft square and 12.5 ft long with perforated, variable porosity (0.5- to 10-percent open) walls. It is completely enclosed in a plenum chamber from which the air can be evacuated, allowing part of the tunnel airflow to be removed through the perforated walls of the test section.

For store separation testing, two separate and independent support systems are used to support the models. The parent-aircraft model is inverted in the test section and supported by an offset sting attached to the main pitch sector. The store model is supported by the CTS which extends down from the tunnel top wall and provides store movement (six degrees of freedom) independent of the parent-aircraft model. An isometric drawing of a typical store separation installation is shown in Fig. 1, Appendix I.

Also shown in Fig. 1 is a block diagram of the computer control loop used during captive trajectory testing. The analog system and the digital computer work as an integrated unit and, utilizing required input information, control the store movement during a trajectory. Store positioning is accomplished by use of six individual d-c electric motors. Maximum translational travel of the CTS is  $\pm 15$  in. from the tunnel centerline in the lateral and vertical directions and 36 in. in the axial direction. Maximum angular displacements are  $\pm 45$  deg in pitch and yaw and  $\pm 360$  deg in roll. A more complete description of the test facility can be found in Ref. 1. A schematic showing the test section details and the location of the models in the tunnel is shown in Fig. 2.

## 2.2 TEST ARTICLE

The test articles were 0.05-scale models of the F-4C parent aircraft and the LAU-69/A rocket launcher (full and empty). A sketch showing the basic dimensions of the F-4C parent model is presented in Fig. 3. Details and dimensions of the centerline and inboard pylons are shown in Fig. 4, the 370-gal fuel tank and outboard pylon are shown in Fig. 5, the Triple Ejection Rack (TER) is shown in Fig. 6, the Multiple Ejection Rack (MER) is shown in Fig. 7, and the LAU-69/A models are shown in Figs. 8 and 9.

The LAU-69/A empty metric model is shown in a cutaway view in Fig. 9a. In an attempt to minimize the blockage of the balance on the flow through the launcher tubes, the tubes were opened into a plenum near the front of the model. The flow was then ducted to the balance cavity where it passed over the balance and out the base of the model. A thin mylar film (0.00025 in. thick) was used to keep the flow through the balance cavity from impinging directly on the balance. The nose section with the launcher tubes was removable, and for the cases run with the launcher tubes blocked, the nose section was replaced with one without holes.

The F-4 parent model is geometrically similar to the full-scale airplane except for some modifications incident to wind-tunnel installations and CTS operation. The tail section was removed because of interference with the CTS support movement. The parent model was inverted in the tunnel and attached by a 20-deg offset sting to the main sting support system (Fig. 2). The TER and MER were mounted on the inboard and centerline pylons, respectively, and were aligned with the 30-in. suspension lug positions as indicated in Figs. 4, 6, and 7. The MER was installed in both forward and aft positions as indicated in Fig. 7. Figure 10 shows the numbering sequence of the TER and MER stations and the roll orientations of the stores mounted on each of the launch positions. Figure 11 shows a typical tunnel installation photograph of the parent aircraft and store model.

## 2.3 INSTRUMENTATION

A five-component internal strain-gage balance was used to obtain store aerodynamic force and moment data. Translational and angular positions of the store were obtained from CTS analog outputs, while parent-model angle of attack was determined by an angular position indicator on the main pitch sector. The right-wing and center line pylons contained a touch wire system which enabled the store to be accurately positioned for launch. The system was also wired to automatically stop the CTS motion and give visual indication should the store or sting support make contact with any surface other than the touch wire.

## SECTION III TEST DESCRIPTION

### 3.1 TEST CONDITIONS

Separation trajectory data were obtained at Mach numbers from 0.29 to 0.78. Table I (Appendix II) presents the tunnel dynamic pressures at which the trajectories were obtained. The tunnel conditions were held constant at the desired Mach number and stagnation pressure while data for each trajectory were obtained.

Because of the large angles encountered during the trajectories, the mechanical limits or sting grounds often determined when the trajectory stopped. A few trajectories were stopped after enough data on that particular trajectory were obtained to indicate a trend.

### 3.2 TRAJECTORY DATA ACQUISITION

To obtain a trajectory, test conditions were established in the tunnel and the parent model was positioned at the desired angle of attack. The store model was then oriented to a position corresponding to the store carriage location. After the store was set at the desired initial position, operational control of the CTS was switched to the digital computer which controlled the store movement during the trajectory through commands to the CTS analog system (see block diagram Fig. 1). Data from the wind tunnel, consisting of measured model forces and moments, wind-tunnel operating conditions, and CTS rig positions, were input to the digital computer for use in the full-scale trajectory calculations.

The digital computer was programmed to solve the six-degree-of-freedom equations to calculate the angular and linear displacements of the store relative to the parent-aircraft pylon (Ref. 2). In general, the program involves using the last two successive measured values of each static aerodynamic coefficient to predict the magnitude of the coefficients over the next time interval of the trajectory. These predicted values are used to calculate the new position and attitude of the store at the end of the time interval. The CTS is then commanded to move the store model to this new position and the aerodynamic loads are measured. If these new measurements agree with the predicted values, the process is continued over another time interval of the same magnitude. If the measured and predicted values do not agree within the desired precision, the calculation is repeated over a time interval one-half the previous value. This process is repeated until a complete trajectory has been obtained.

In applying the wind-tunnel data to the calculations of the full-scale store trajectories, the measured forces and moments are reduced to coefficient form and then applied with proper full-scale store dimensions and flight dynamic pressure. Dynamic pressure was calculated using a flight velocity equal to the free-stream velocity component plus the components of store velocity relative to the aircraft, and a density corresponding to the simulated altitude.

The initial portion of each launch trajectory incorporated simulated ejector forces in addition to the measured aerodynamic forces acting on the store. The ejector force

functions for the stores are presented in Fig. 12. The ejector force was considered to act perpendicular to the rack mounting surface. The locations of the applied ejector forces and other full-scale store parameters used in the trajectory calculations are listed in Table II, Appendix II.

### 3.3 CORRECTIONS

Balance, sting, and support deflections caused by the aerodynamic loads on the store models were accounted for in the data reduction program to calculate the true store-model angles. Corrections were also made for model weight tares to calculate the net aerodynamic forces on the store model.

### 3.4 PRECISION OF DATA

The trajectory data are subject to error from several sources including tunnel conditions, balance measurements, extrapolation tolerances allowed in the predicted coefficients, computer inputs, and CTS position control, which was  $\pm 0.05$  in. for the translational settings and  $\pm 0.15$  deg for angular displacement settings in pitch and yaw. Extrapolation tolerances were  $\pm 0.10$  for each of the aerodynamic coefficients. The maximum uncertainties in full-scale position data caused by balance precision limitations are given below. The maximum uncertainties for the static data are also given below. The estimated uncertainty in setting Mach number was no greater than  $\pm 0.002$  and the uncertainty in parent-model angle of attack was estimated to be  $\pm 0.1$  deg.

#### MAXIMUM TRAJECTORY UNCERTAINTIES

<u>Model Configuration</u>	<u>t, sec</u>	<u>x, ft</u>	<u>y, ft</u>	<u>z, ft</u>	<u><math>\theta</math>, deg</u>	<u><math>\psi</math>, deg</u>
Empty	0.3	$\pm 0.30$	$\pm 0.40$	$\pm 0.20$	$\pm 8.0$	$\pm 12.0$
Full	0.3	$\pm 0.04$	$\pm 0.05$	$\pm 0.02$	$\pm 2.0$	$\pm 2.0$

#### MAXIMUM UNCERTAINTIES IN STATIC STABILITY AND AXIAL FORCE COEFFICIENTS

<u><math>C_Y</math></u>	<u><math>C_n</math></u>	<u><math>C_A</math></u>
$\pm 0.017$	$\pm 0.030$	$\pm 0.014$

## SECTION IV RESULTS AND DISCUSSION

### 4.1 GENERAL

Trajectories were obtained to determine the safe separation envelopes of the full and empty LAU-69/A launcher from the F-4C aircraft. Included were two full configurations simulating loads of the 2.75-in. folding fin rockets with heavy and light warheads,

respectively. No attempt will be made in this report to establish the safe separation envelopes or qualify the store as safe or unsafe for aircraft separation.

The results obtained during the test consisted of ejector-separated trajectories simulating release from right- and left-wing inboard pylons and the centerline pylon. All TER separation sequences not in the 1, 2, 3 order represent left-wing simulations. From the centerline, trajectories were simulated for launch from MER locations 2, 4, and 6. In order to simplify the test procedure, the centerline symmetry of the model was used and all trajectories which would have been launched from station 4 were launched from station 6 with a dummy store on station 4. For the TER trajectories, the MER was in either the forward or aft location (Fig. 7). The aft MER position was used for all MER trajectories. Plots showing the linear displacements of the stores relative to the carriage positions and the angular displacements relative to the flight-axis system are presented in Figs. 13 through 16 and Fig. 18. Positive X, Y, and Z displacements (as seen by the pilot) are forward, to the right, and down, respectively. Positive changes in  $\theta$  and  $\psi$  (as seen by the pilot) are nose up and nose to the right, respectively. Table II lists the full-scale store parameters used in the trajectory calculations and Table III describes the aircraft load configuration nomenclature.

#### 4.2 LAU-69/A, FULL

Trajectory data for the full LAU-69/A with heavy and light warheads are presented in Figs. 13 and 14, respectively. The location of the ejector foot aft of the store center-of-gravity (Table II) would be expected to cause the store to pitch or yaw its nose toward the TER or MER rack initially. Since the store was statically unstable, the initial rotation caused by the ejector foot continued (typical examples—Fig. 14a below  $M_\infty = 0.62$  for  $\theta$  and 13b and c for  $\psi$ ) except where the local flow field angle was large enough to cause the aerodynamic moment to overcome the moment produced by the ejector force. The Mach number at which the direction of pitch or yaw changed because of local flow field effects varied according to configuration (light or heavy warhead) and station on the TER or MER, but generally was between  $M_\infty = 0.53$  and 0.70. For example, at  $M_\infty = 0.62$ ,  $\alpha = 2.3$  the store with heavy warheads pitched up (Fig. 13a), while the store with the light warheads pitched down (Fig. 14a). For the heavy warhead, the center-of-gravity was farther forward which increased the moment applied by the ejector foot. Trajectories from the MER stations showed the same trends as those from the TER, except that the local flow field effects appeared to be shifted to higher angles of attack and lower Mach numbers than for the TER. For example, at  $M_\infty = 0.53$ ,  $\alpha = 3.5$ , from the TER on the inboard pylon, the store pitched up (Fig. 14a), while from the MER on the centerline the store pitched down (Fig. 14g).

The trajectories in Figs. 13 and 14 from the TER are for the MER located in two different positions, forward and aft (see Fig. 7). A few trajectories were run with the MER in both locations to assess the effect of MER location. The comparison data including repeat runs at  $M_\infty = 0.78$  with the MER in forward and aft locations are presented in Fig. 15. In Fig. 15a and b for Station 2 of the TER, not much effect is shown, while in Fig. 15c for Station 3 of the TER, a difference is evident. The effect in Fig. 15c appears to be one of changing the Mach number at which  $\theta$  and  $\psi$  reverse directions.



### 4.3 LAU-69/A, EMPTY

The trajectories for the empty LAU-69/A are presented in Fig. 16. With the munitions expended, the center-of-gravity of the store lay aft of the ejector foot. The moment produced by the ejector foot tended to rotate the store nose away from the TER or MER. The empty launcher was statically unstable and therefore tended to continue to rotate in the direction the ejector foot initiated. For the inboard shoulder (Station 2) of the TER, the local flow field angularity was great enough to produce an aerodynamic moment to overcome the initial moment produced by the ejector foot, and reversed the angular movement in yaw ( $\psi$ ) (Fig. 16b and f).

### 4.4 COMPARISON OF EMPTY LAUNCHER WITH TUBES OPEN AND CLOSED

In the past, tests with empty launchers have been conducted with the launcher tubes either open or closed to a through-flow of air. The fabrication of the models with the launcher tubes open presents many problems. In an effort to determine whether the launcher tubes must be simulated or whether a closed flat-face launcher would be adequate, static stability and axial-force data (Fig. 17) and trajectory data (Fig. 18) were obtained. The side-force coefficients are larger for any given yaw angle for the open-tube configuration than for the closed-tube configuration, while the axial-force coefficients are larger for the closed tubes. Significant differences in static stability are evident at low angles of attack. The closed-tube configuration is statically stable below about three-degrees yaw angle, while the open-tube configuration is unstable at all angles.

The trajectory data also show differences in  $X$ ,  $\theta$ , and  $\psi$ . The differences between the open- and closed-tube trajectories appear to increase with increasing time. From this limited amount of data it would appear that the difference between open- and closed-tube simulation of the empty launcher justifies building the models with provisions for mass flow through the launcher tubes.

### REFERENCES

1. Test Facilities Handbook (Ninth Edition). "Propulsion Wind Tunnel Facility, Vol. 5." Arnold Engineering Development Center, July 1971.
2. Christopher, J. P. and Carleton, W. E. "Captive-Trajectory Store-Separation System of the AEDC-PWT 4-Foot Transonic Tunnel." AEDC-TR-68-200 (AD839743), September 1968.

**APPENDIXES**  
**I. ILLUSTRATIONS**  
**II. TABLES**

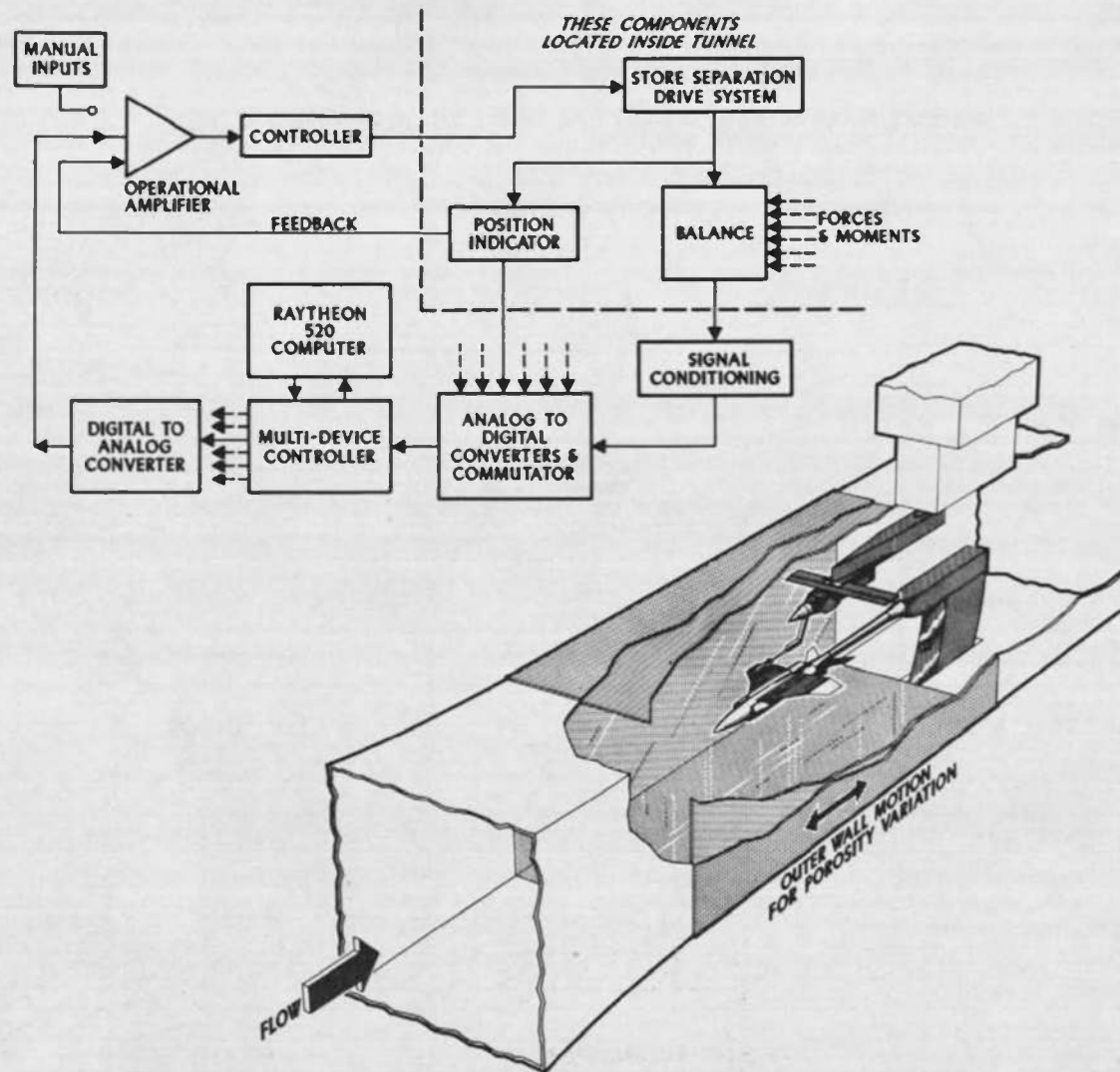
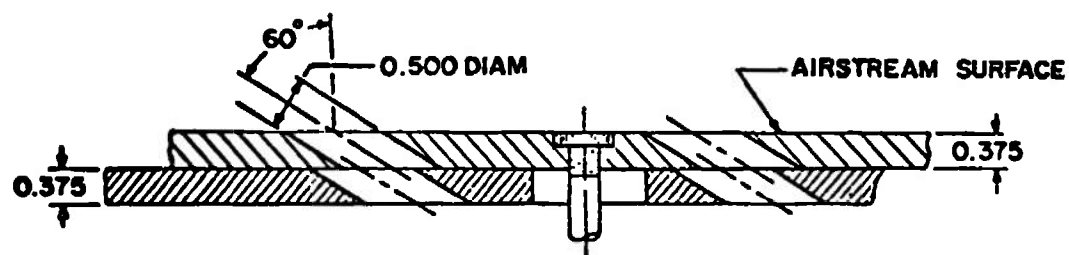


Fig. 1 Isometric Drawing of a Typical Store Separation Installation and a Block Diagram of the Computer Control Loop



TYPICAL PERFORATED WALL CROSS SECTION

NOTE: TUNNEL STATIONS AND DIMENSIONS ARE IN INCHES

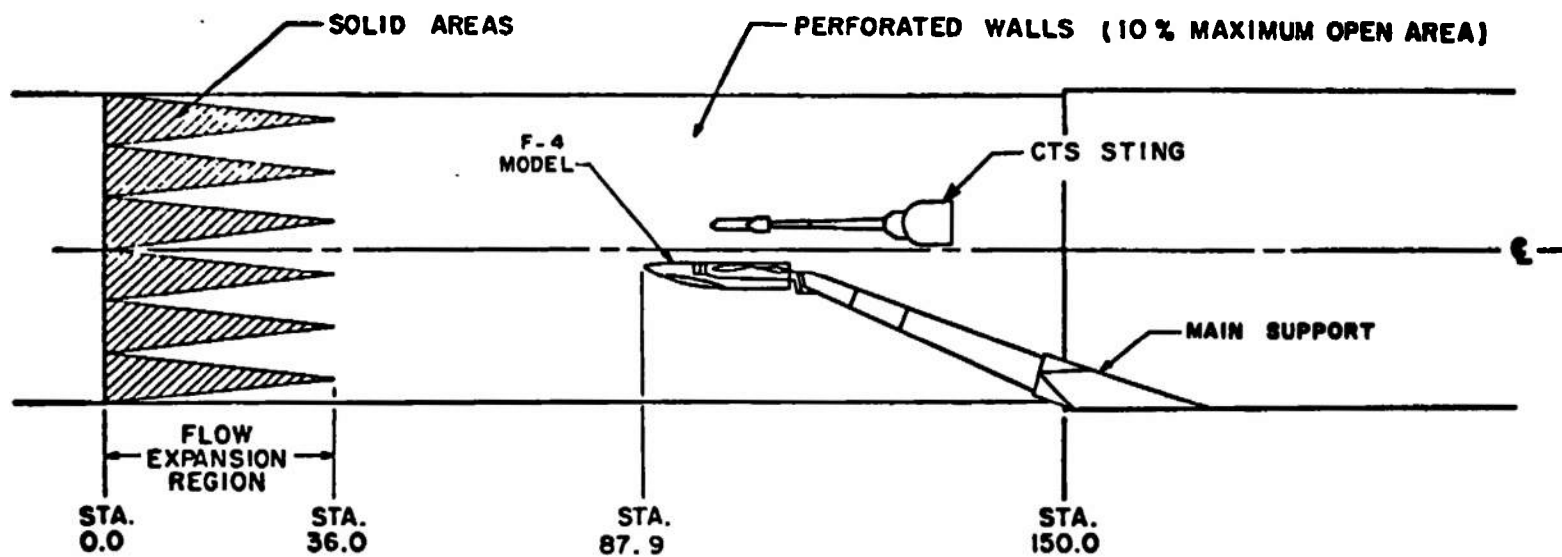


Fig. 2 Schematic of the Tunnel Test Section Showing Model Location

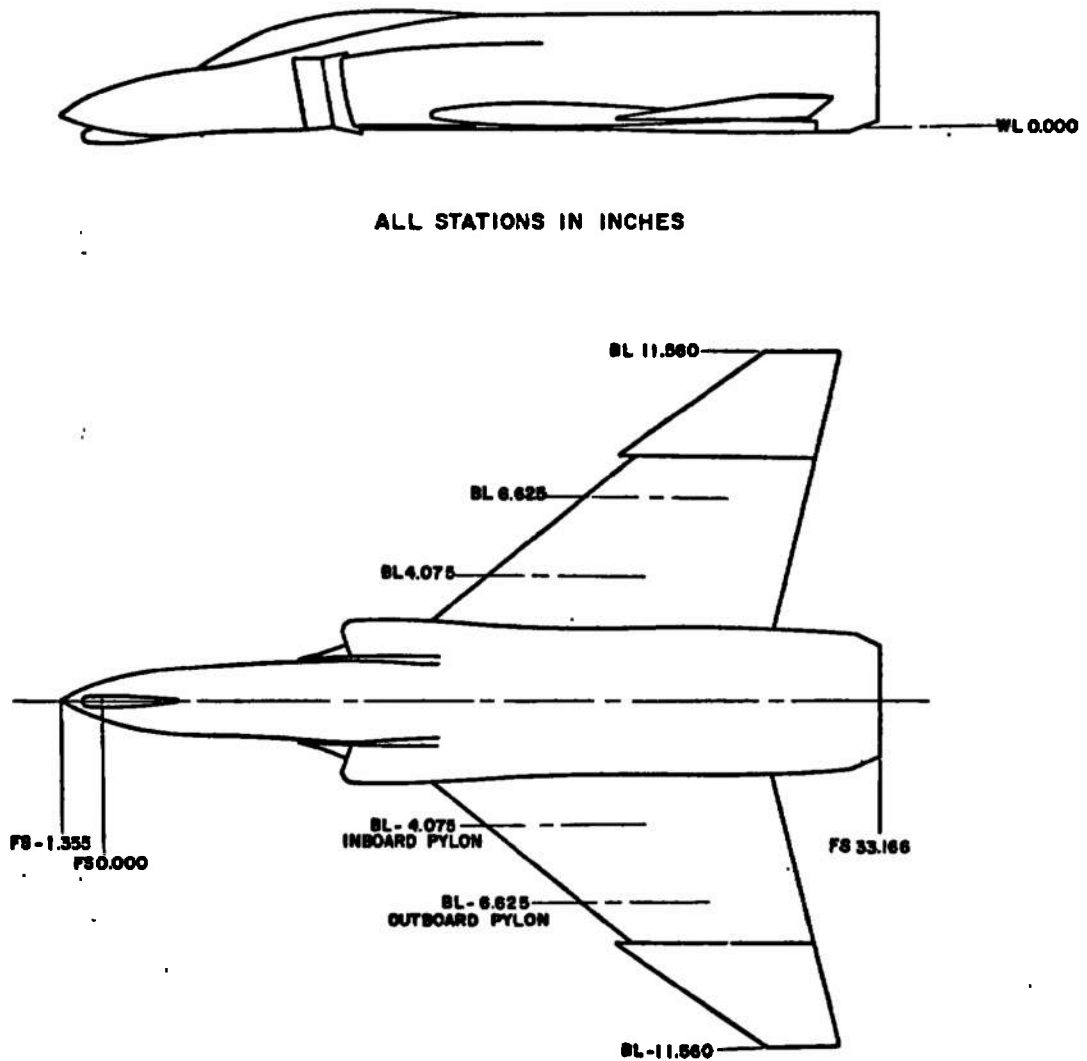
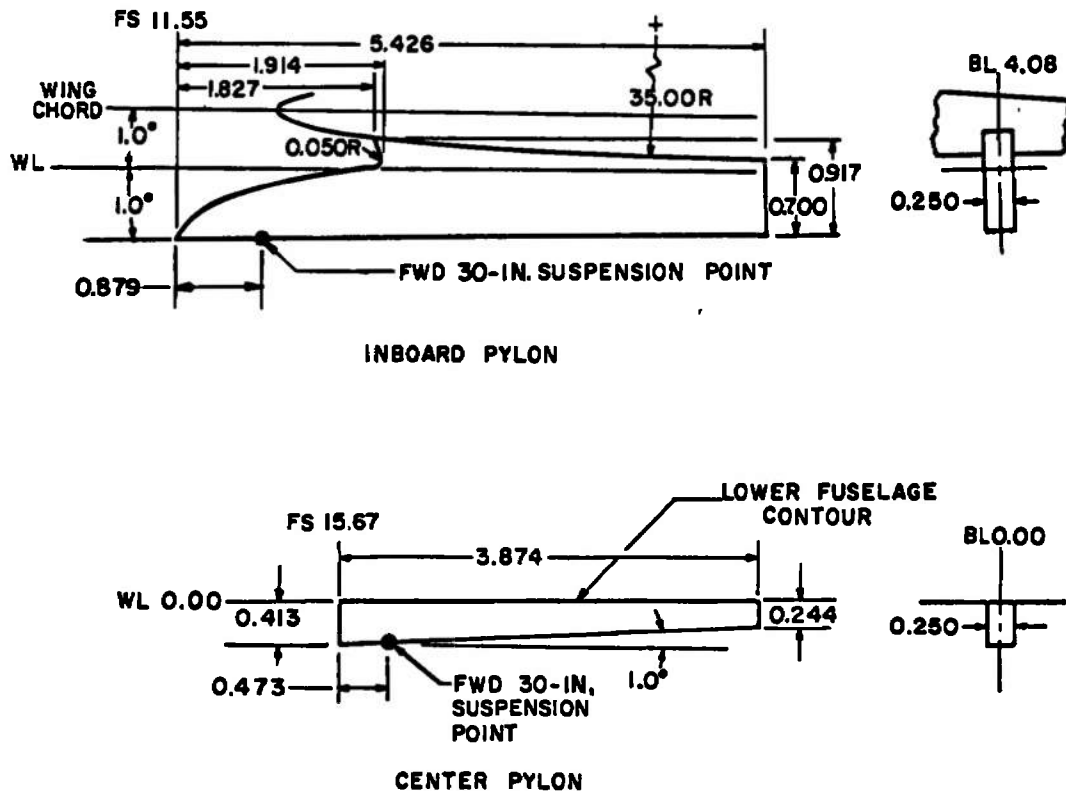
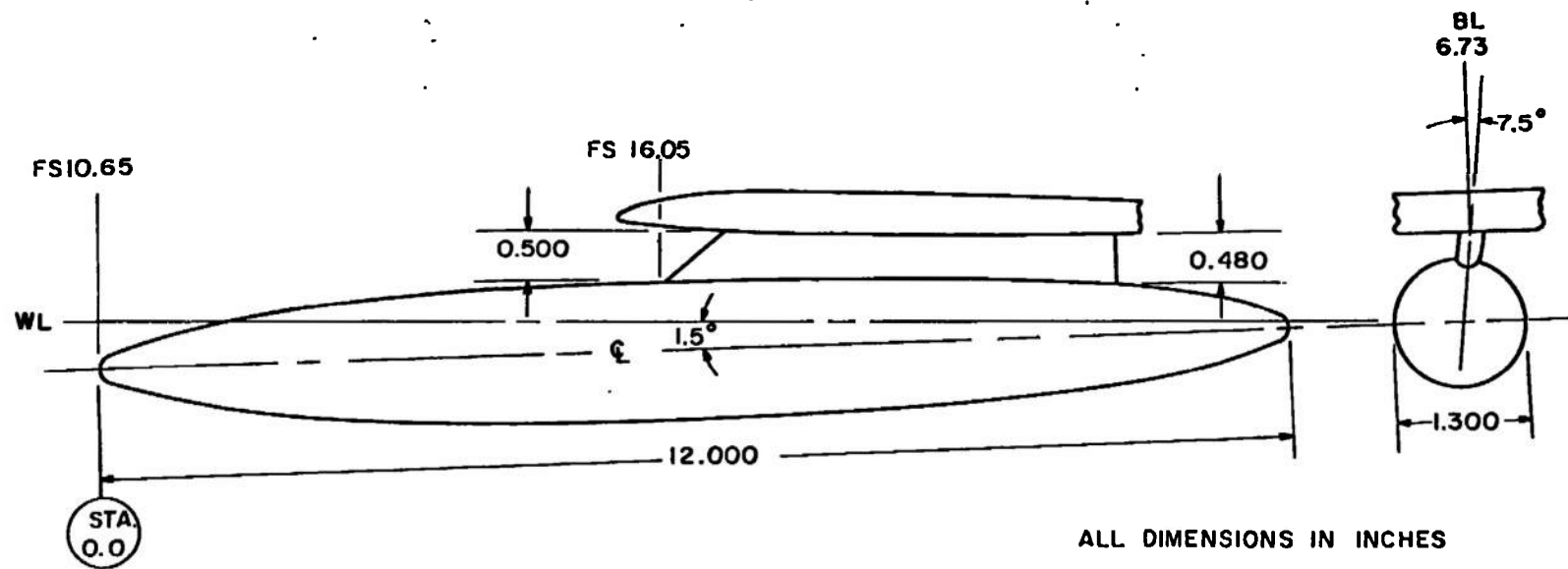


Fig. 3 Sketch of the F-4 Parent-Aircraft Model



ALL DIMENSIONS IN INCHES

Fig. 4 Details and Dimensions of the F-4 Inboard and Centerline Pylon Model



BODY CONTOUR, TYPICAL BOTH ENDS

STATION	BODY DIAM	STATION	BODY DIAM
0.000	0.000	2.500	1.116
0.025	0.100	2.750	1.156
0.050	0.144	3.000	1.190
0.150	0.258	3.250	1.218
0.250	0.340	3.500	1.242
0.500	0.498	3.750	1.260
0.750	0.622	4.000	1.274
1.000	0.724	4.250	1.286
1.250	0.812	4.500	1.294
1.500	0.890	4.750	1.298
1.750	0.958	5.000	1.300
2.000	1.016	6.000	1.300
2.250	1.070		

Fig. 5 Details and Dimensions of the F-4 370-gal Fuel Tank Model

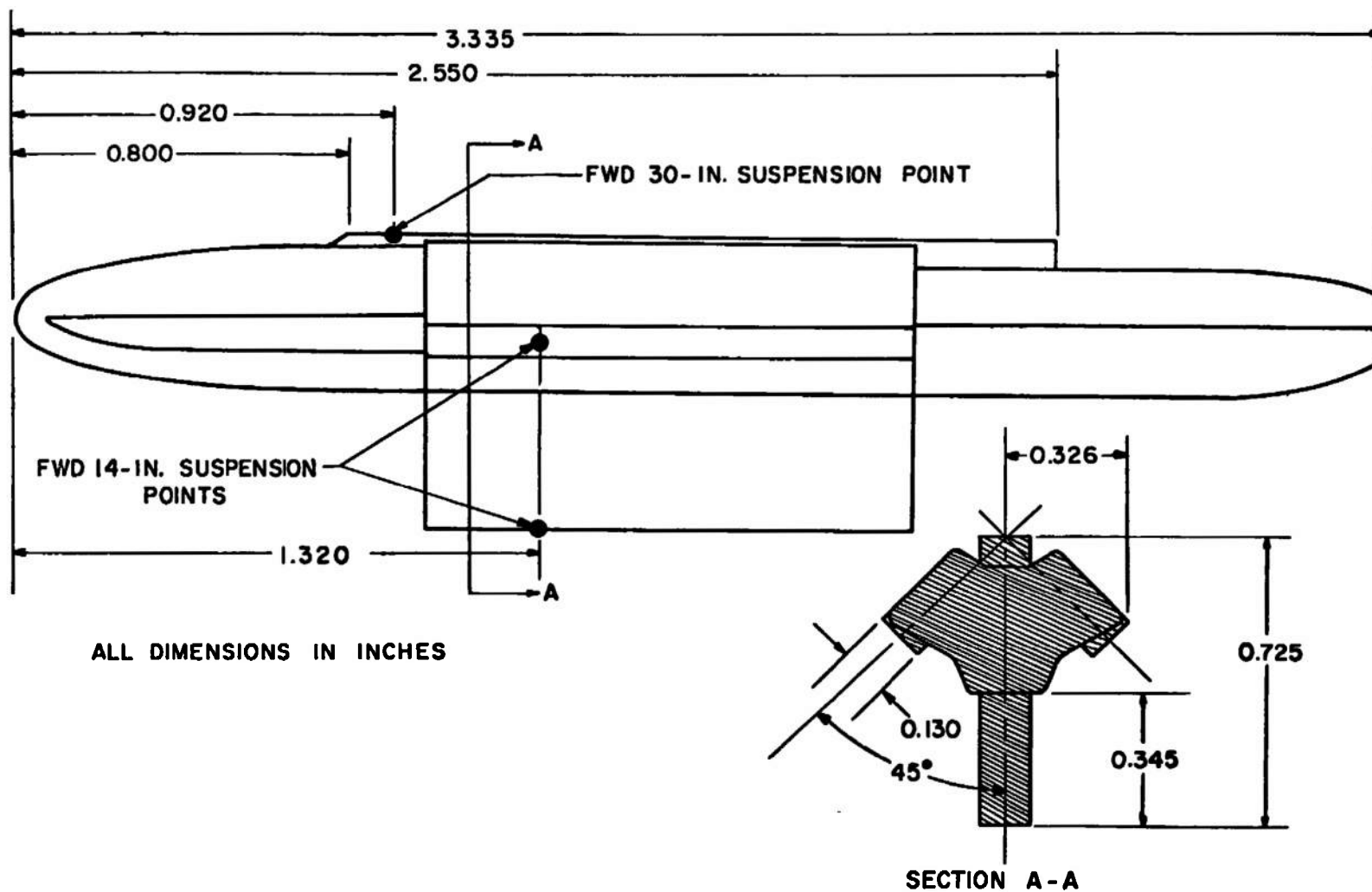


Fig. 6 Details and Dimensions of the TER Model



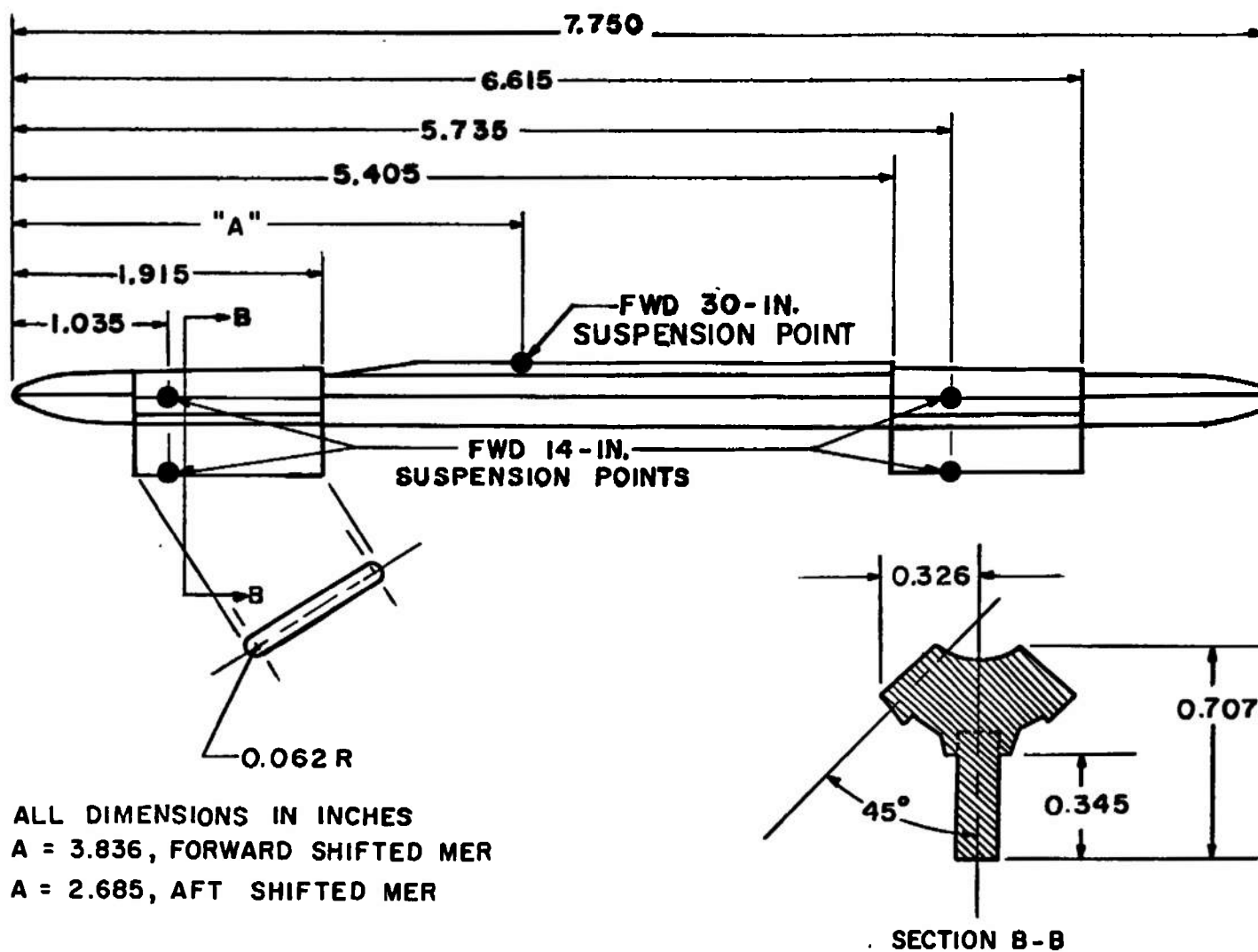
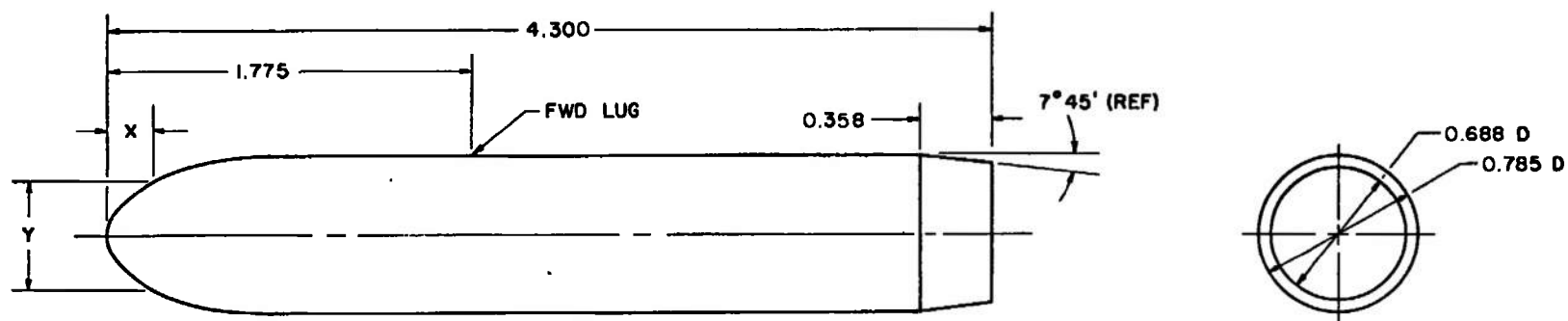


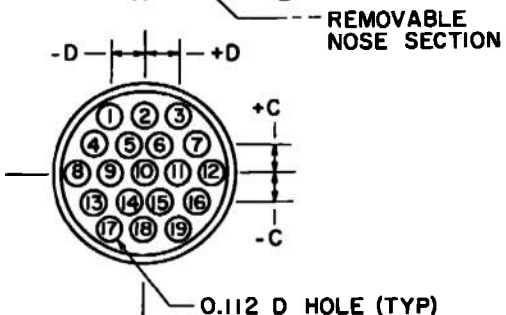
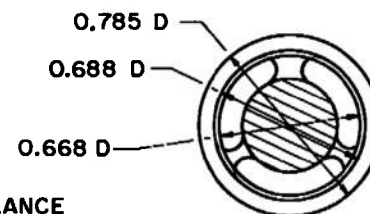
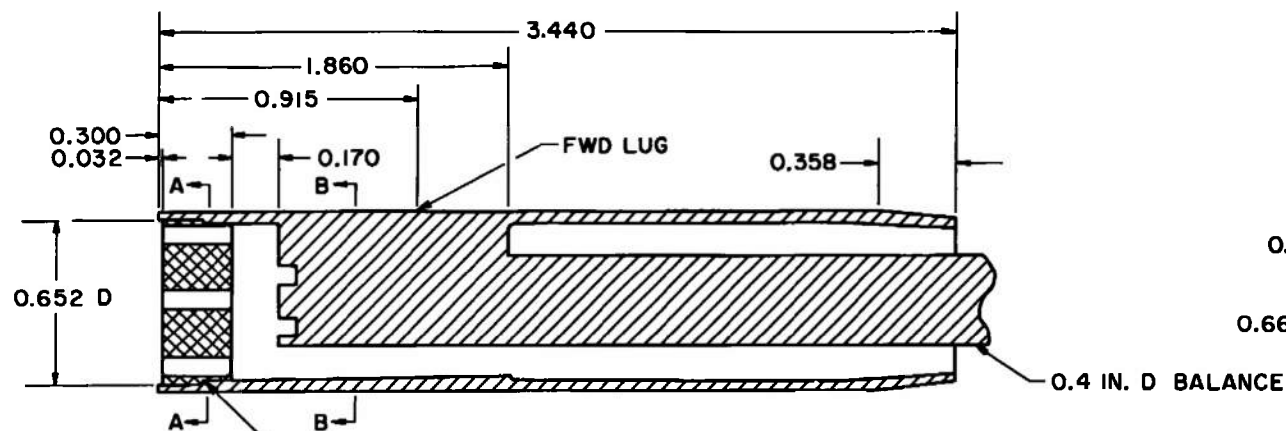
Fig. 7 Details and Dimensions of the MER Model



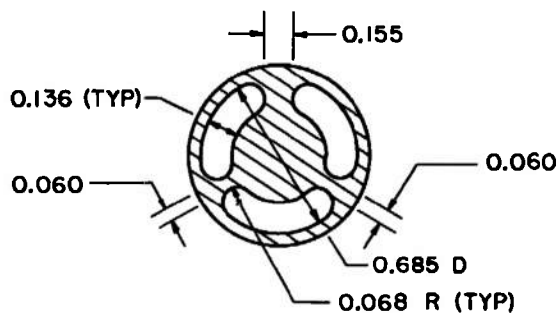
X	Y
0.026	0.201
0.110	0.372
0.240	0.528
0.400	0.645
0.594	0.734
0.800	0.780
0.950	0.785

ALL DIMENSIONS IN INCHES

Fig. 8 Details and Dimensions of the LAU-69/A Metric and Dummy Rocket Launcher Models (Full)



SECTION A-A



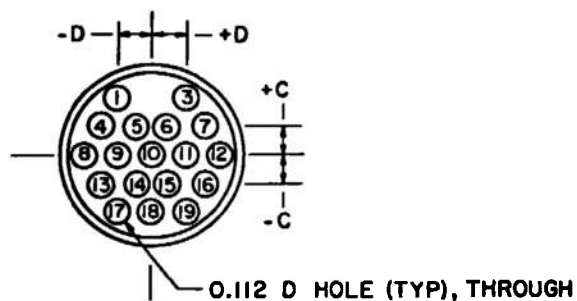
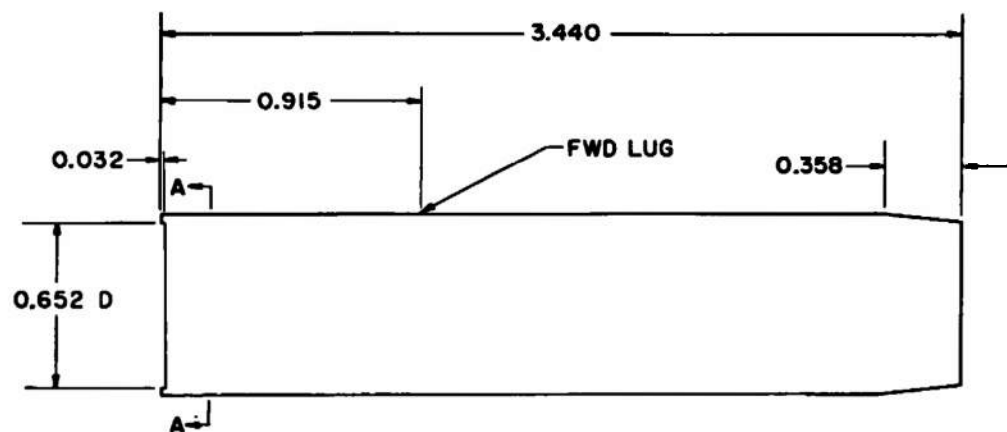
SECTION B-B

ALL DIMENSIONS IN INCHES

HOLE NO.	C	D
1	0.250	-0.143
2	0.250	0.000
3	0.250	0.143
4	0.125	-0.218
5	0.125	-0.062
6	0.125	0.062
7	0.125	0.218
8	0.000	-0.287
9	0.000	-0.143
10	0.000	0.000
11	0.000	0.143
12	0.000	0.287
13	-0.125	-0.218
14	-0.125	-0.062
15	-0.125	0.062
16	-0.125	0.218
17	-0.250	-0.143
18	-0.250	0.000
19	-0.250	0.143

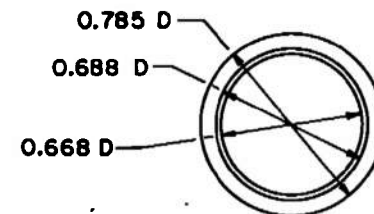
a. Metric Model

Fig. 9 Details and Dimensions of the LAU-69/A Rocket Launcher Models (Empty)



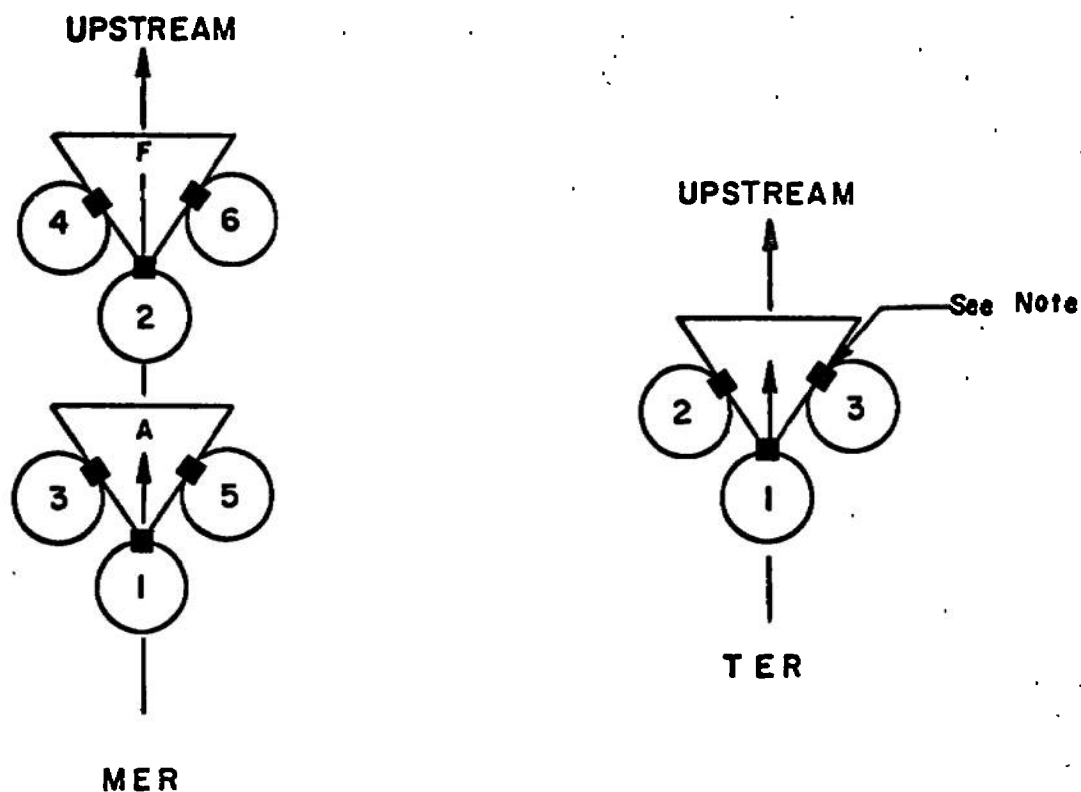
SECTION A-A

ALL DIMENSIONS IN INCHES



HOLE NO.	C	D
1	0.250	-0.143
3	0.250	0.143
4	0.125	-0.218
5	0.125	-0.062
6	0.125	0.062
7	0.125	0.218
8	0.000	-0.287
9	0.000	-0.143
10	0.000	0.000
11	0.000	0.143
12	0.000	0.287
13	-0.125	-0.218
14	-0.125	-0.062
15	-0.125	0.062
16	-0.125	0.218
17	-0.250	-0.143
18	-0.250	0.000
19	-0.250	0.143

b. Dummy Model  
Fig. 9 Concluded



NOTE: The square indicates the orientation of the suspension lugs

TYPE RACK	STATION	ROLL ORIENTATION, deg
MER ↓	1	0
	2	0
	3	45
	4	45
	5	-45
	6	-45
TER ↓	1	0
	2	45
	3	-45

Fig. 10 Schematic of TER and MER Store Stations and Orientations

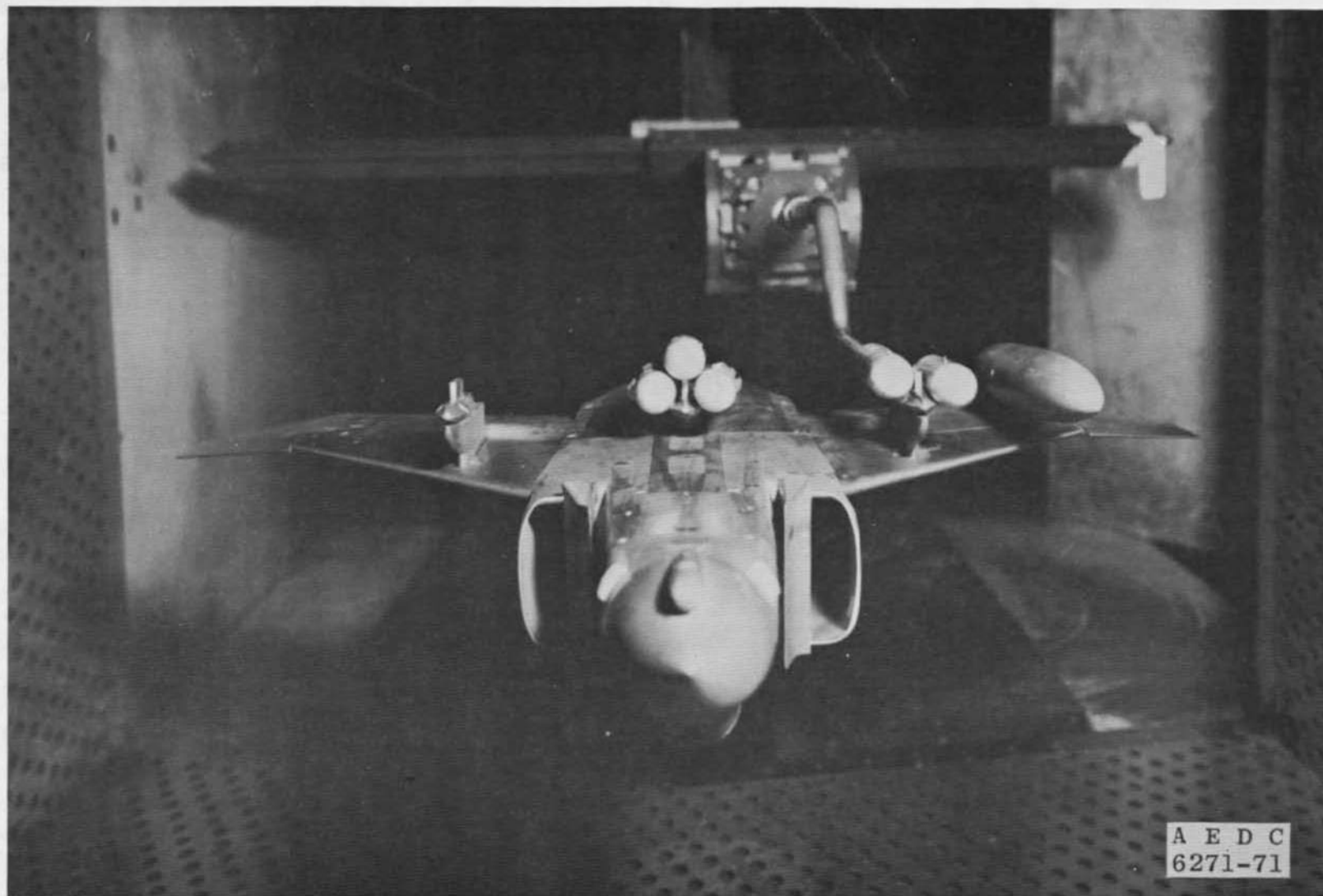
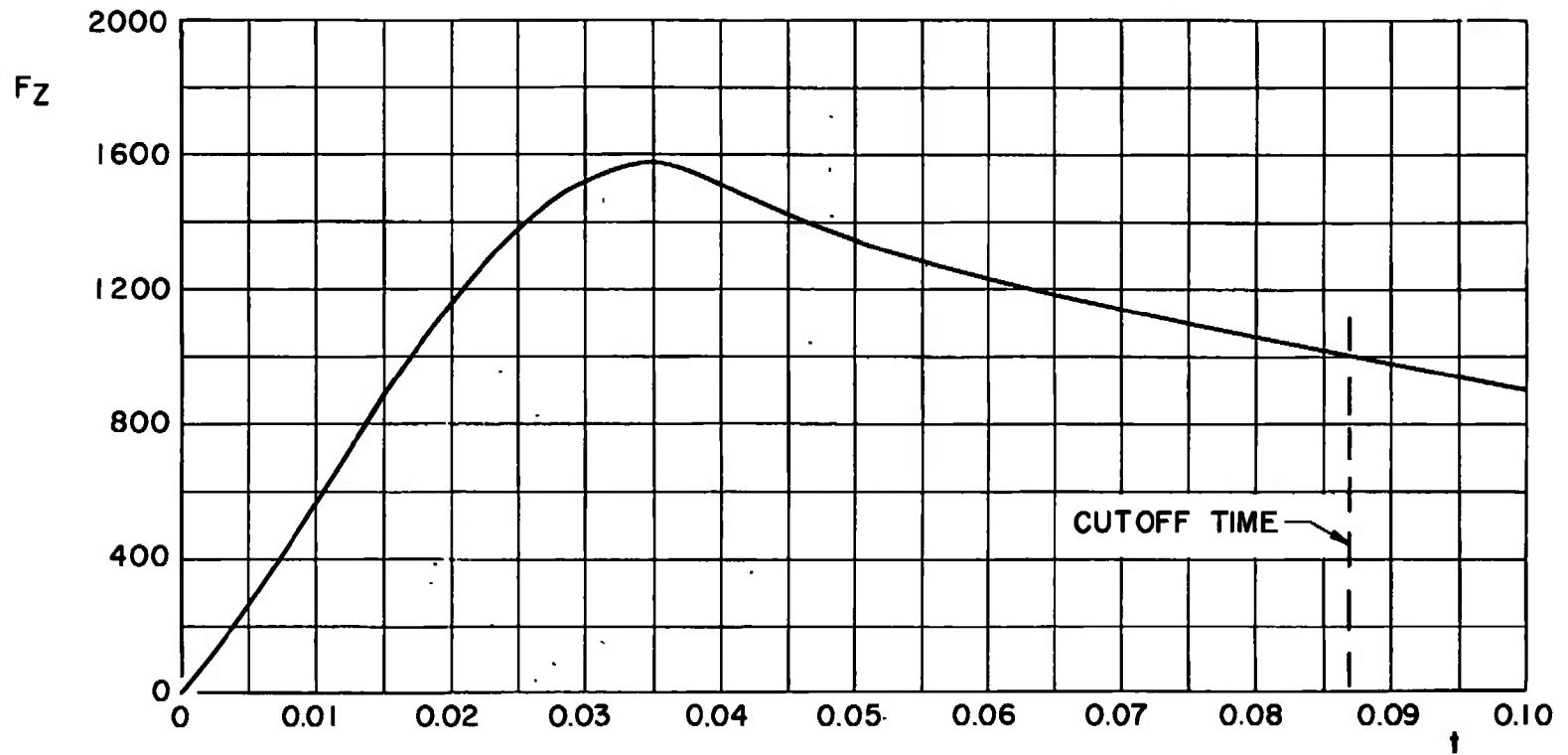
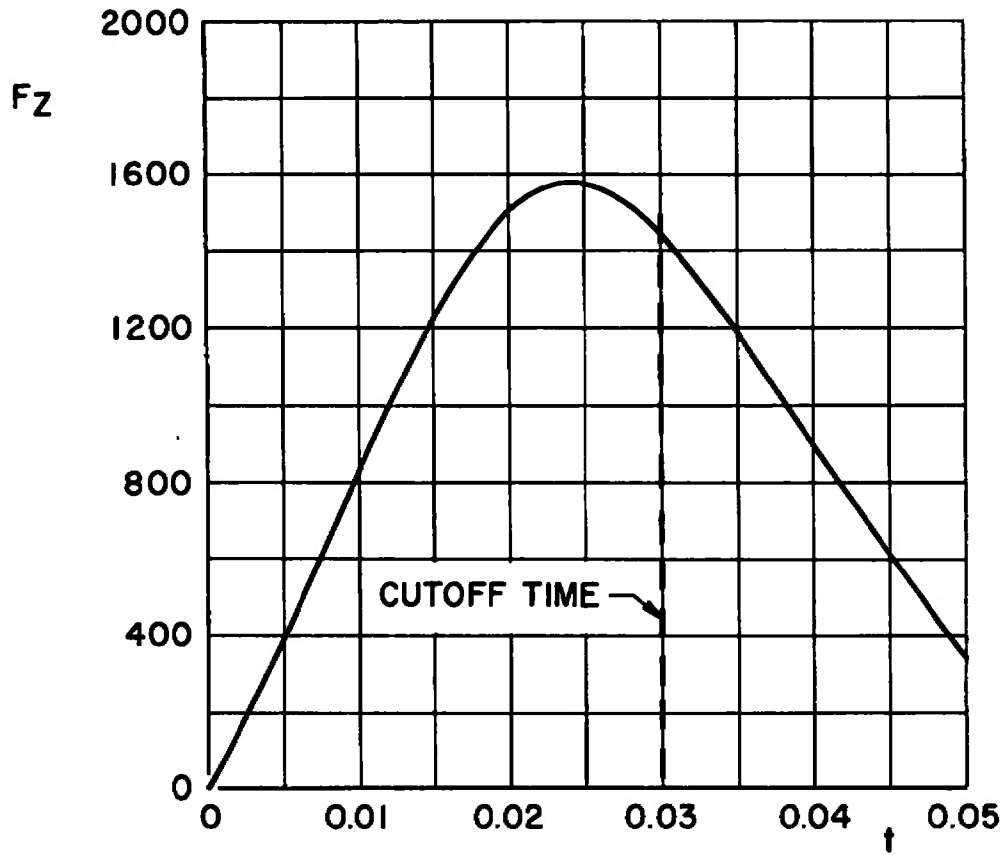


Fig. 11 Tunnel Installation Photograph Showing Parent Aircraft, Store, and CTS

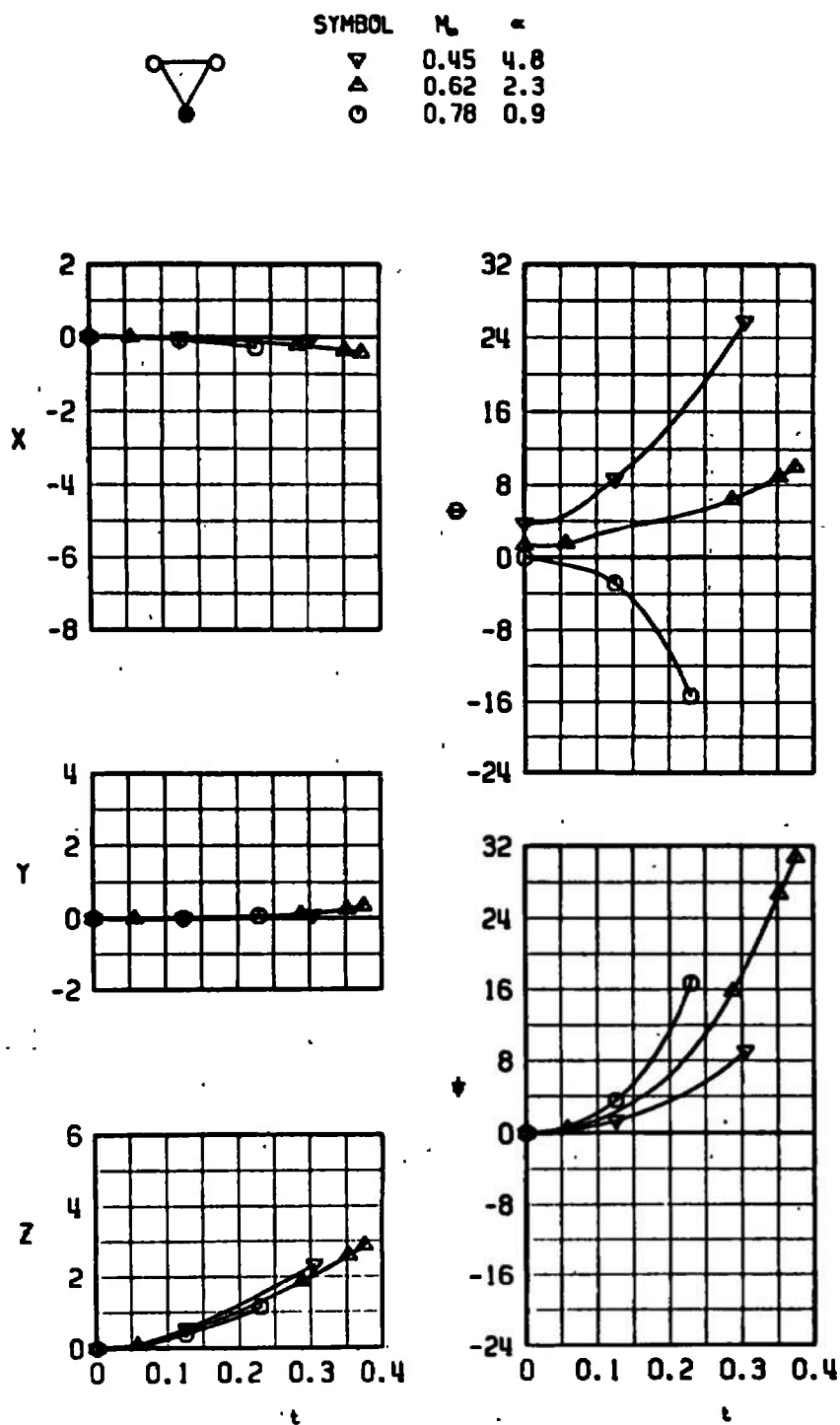


a. LAU-69/A, Full  
 Fig. 12 TER and MER Ejector Force Functions



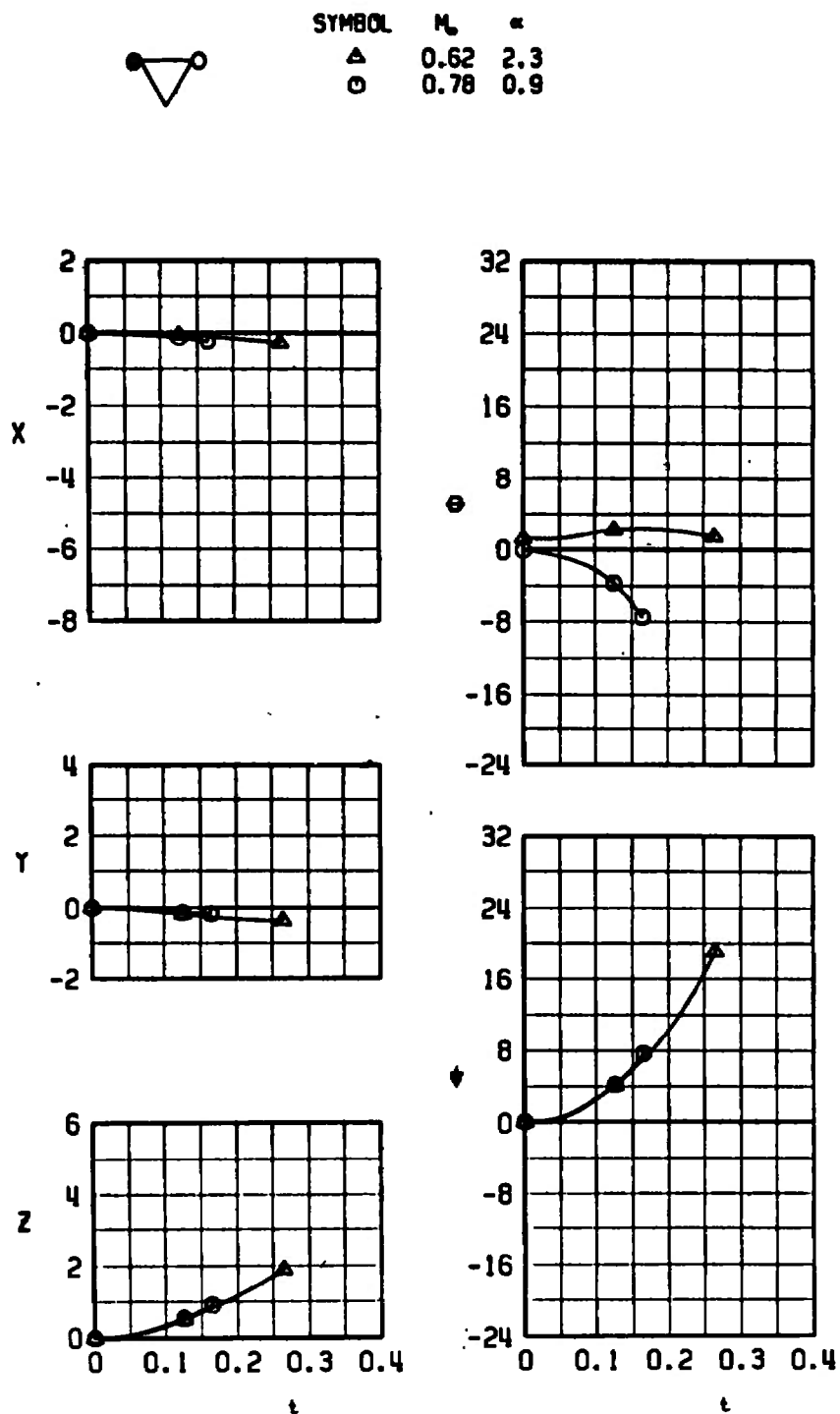
b. LAU-69/A, Empty  
Fig. 12 Concluded





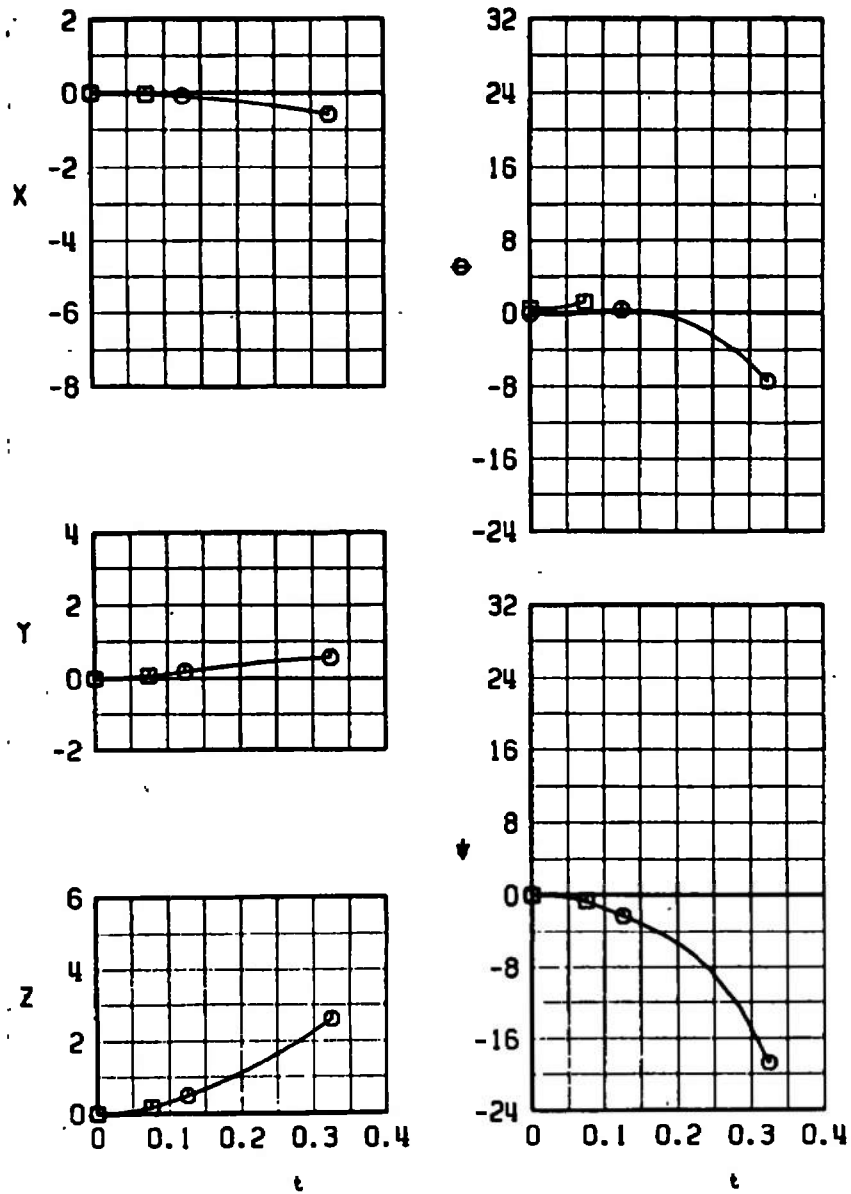
a. TER, Configuration 1H, MER Forward

Fig. 13 Effect of Mach Number on the Separation Characteristics of the LAU-69/A (Full with the Heavy Warhead) from the Inboard TER and Centerline MER

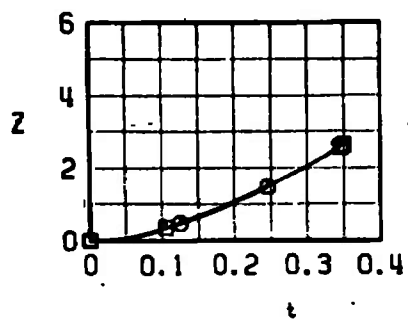
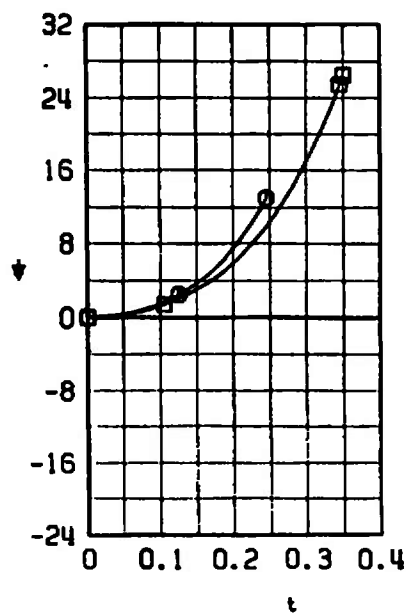
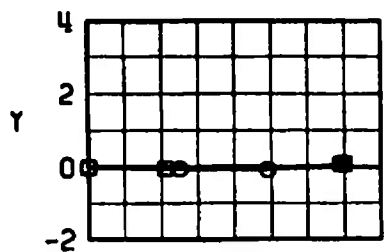
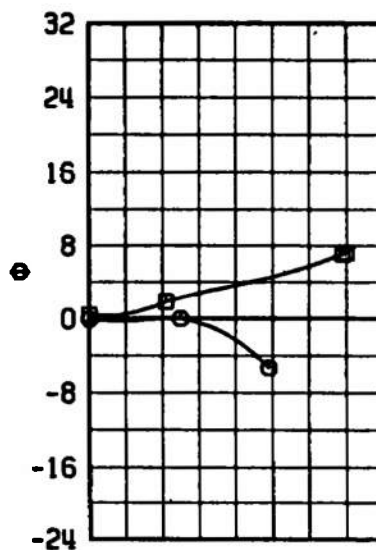
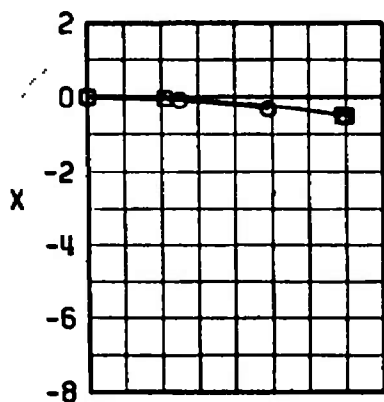
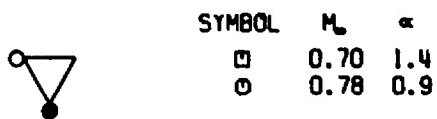


b. TER, Configuration 2H, MER Aft  
Fig. 13 Continued

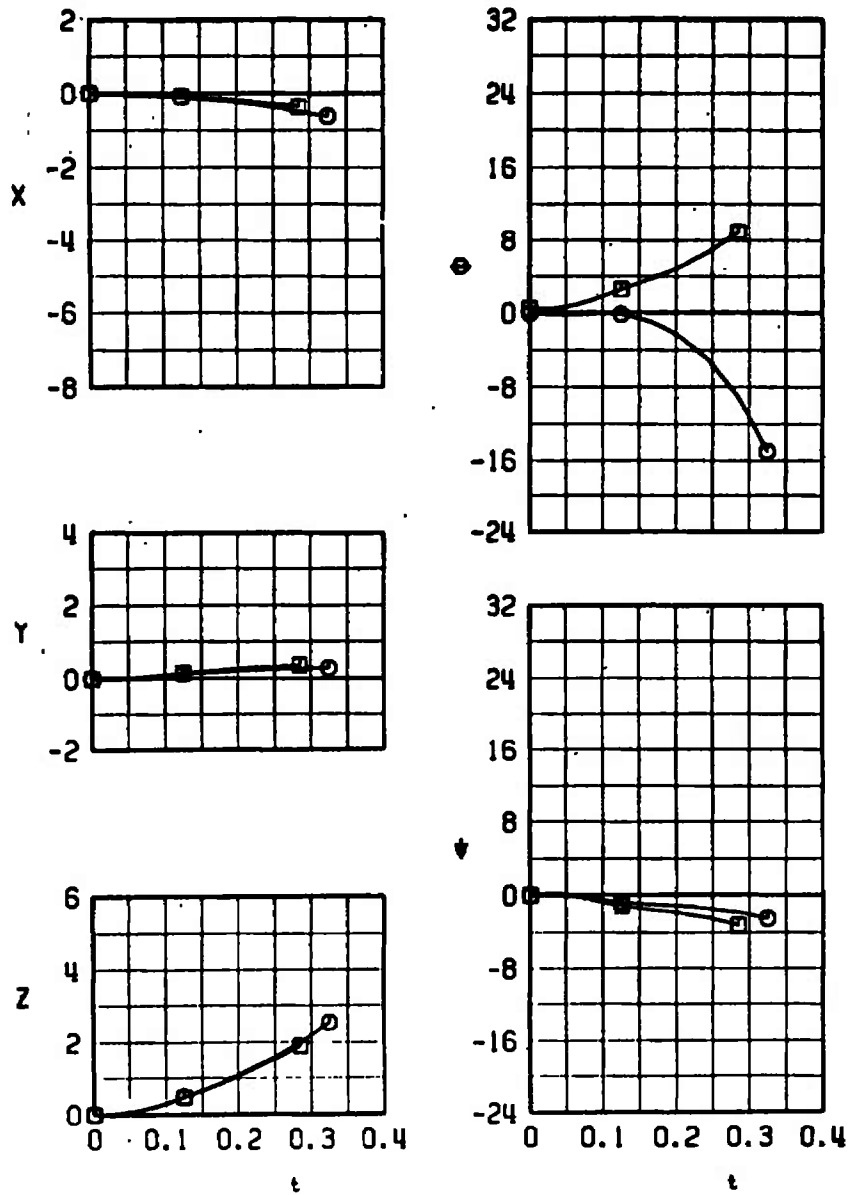
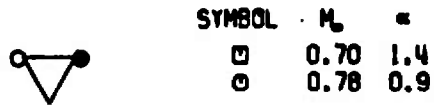
SYMBOL	$M_\infty$	$\alpha$
$\square$	0.70	1.4
$\circ$	0.78	0.9



c. TER, Configuration 3H, MER Forward  
Fig. 13 Continued

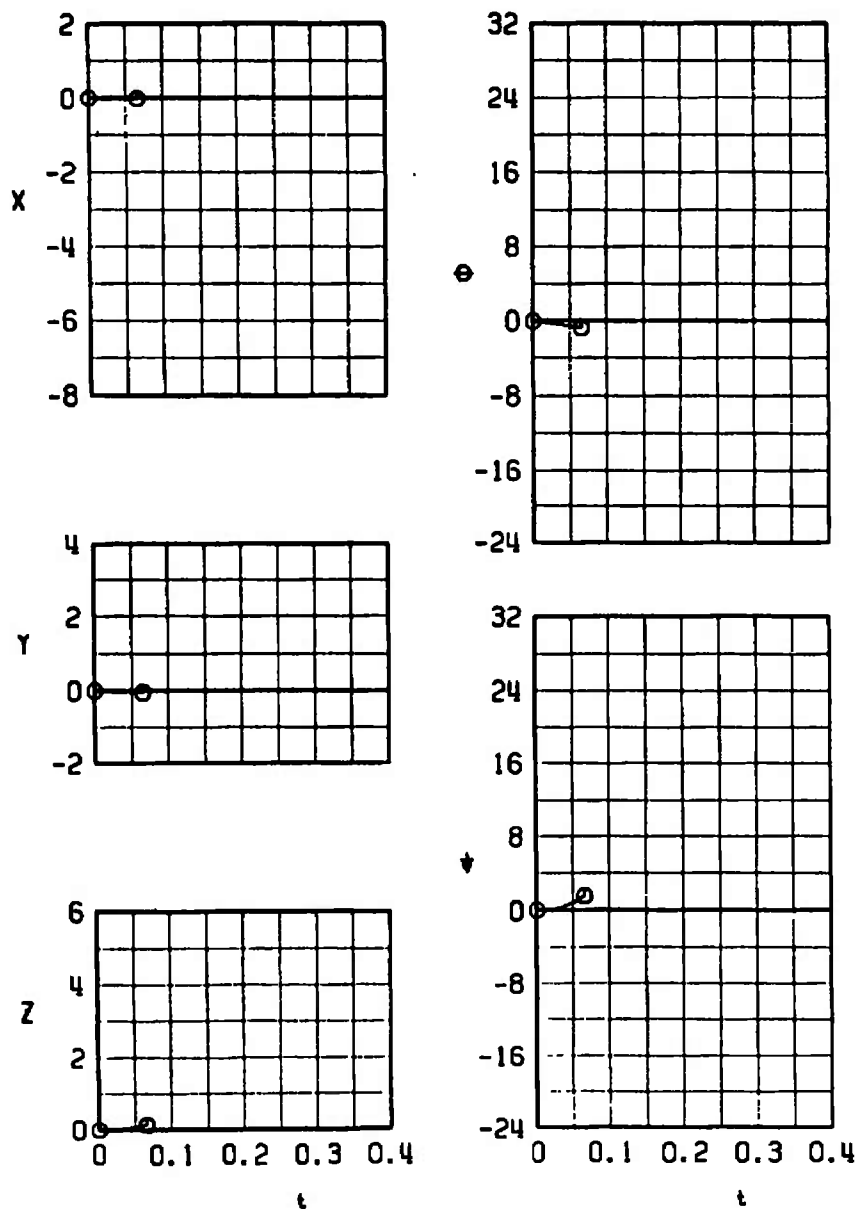


d. TER, Configuration 4H, MER Forward  
Fig. 13 Continued

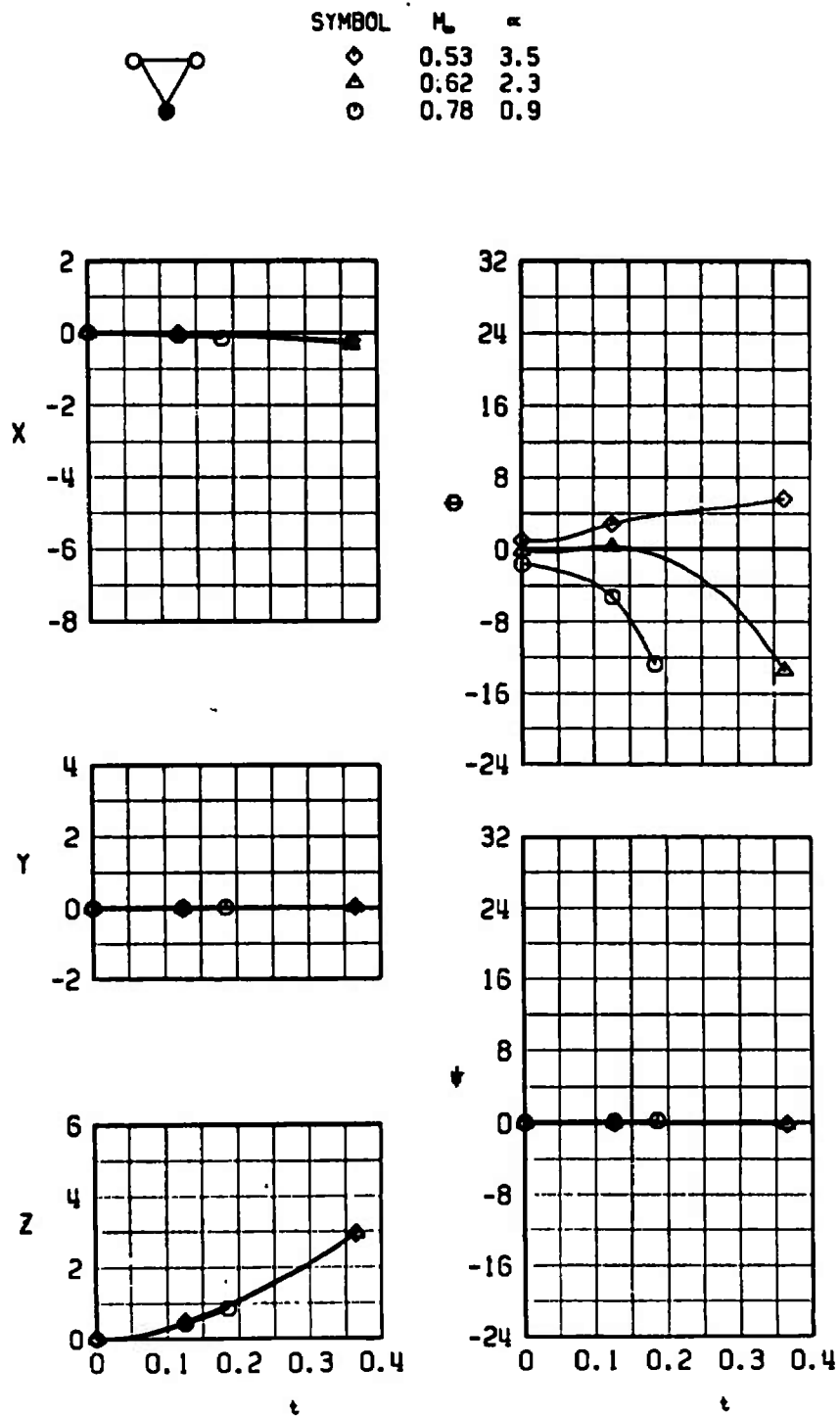


e. TER, Configuration 5H, MER Forward  
Fig. 13 Continued

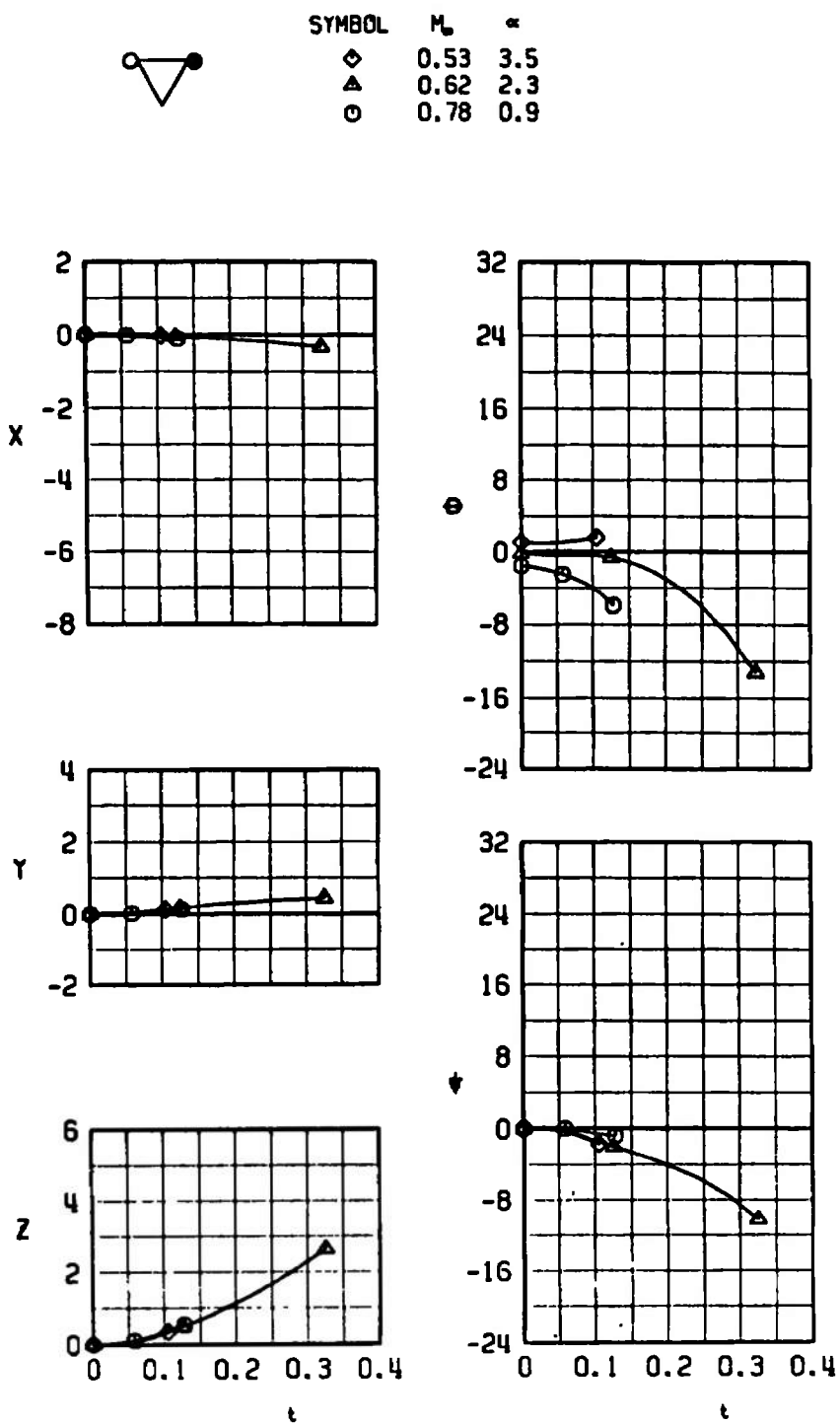
SYMBOL	$M_\infty$	$\alpha$
○	0.78	0.9



f. TER, Configuration 6H, MER Forward  
Fig. 13 Continued

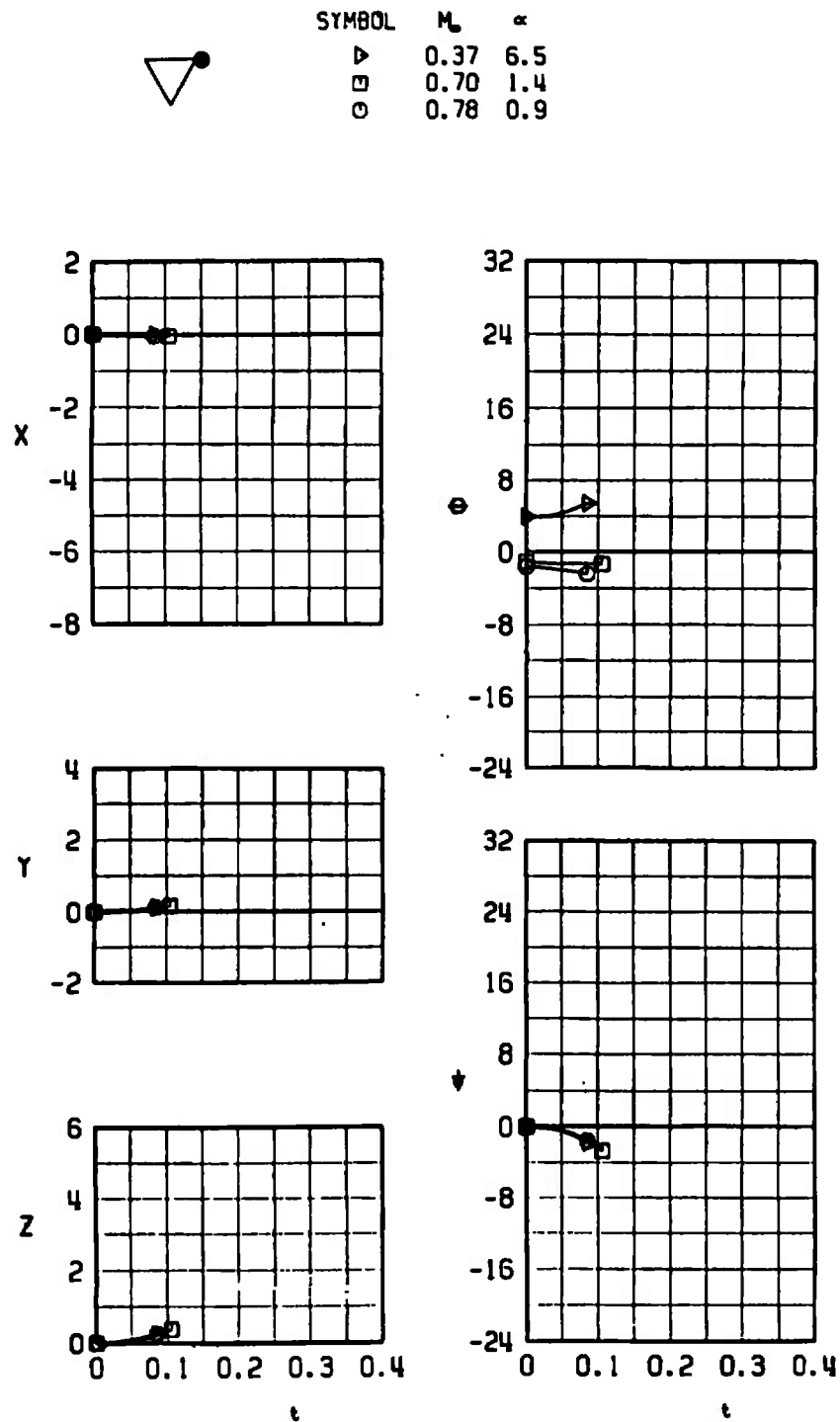


g. MER, Configuration 7H, MER Aft  
Fig. 13 Continued

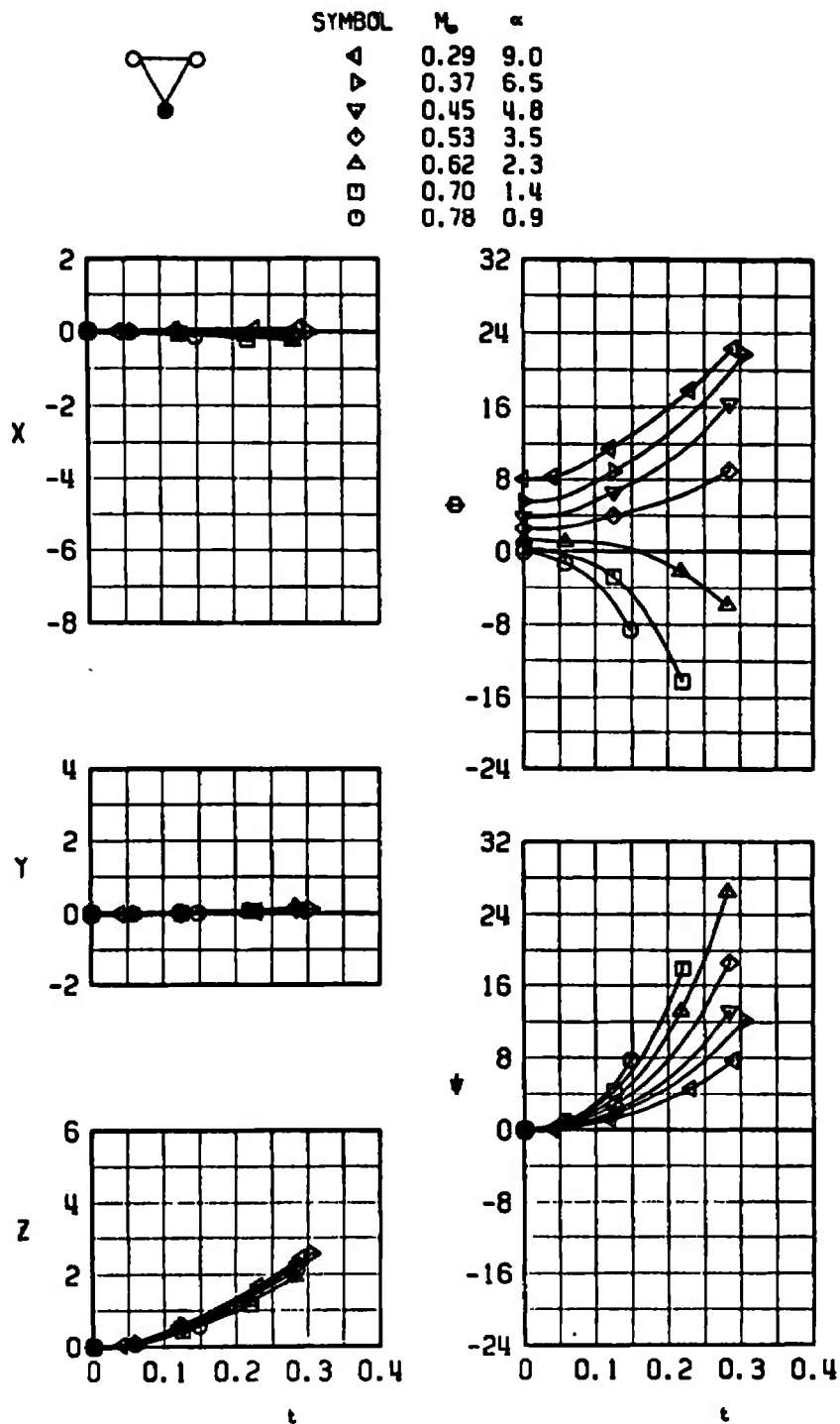


h. MER, Configuration 8H, MER Aft  
Fig. 13 Continued









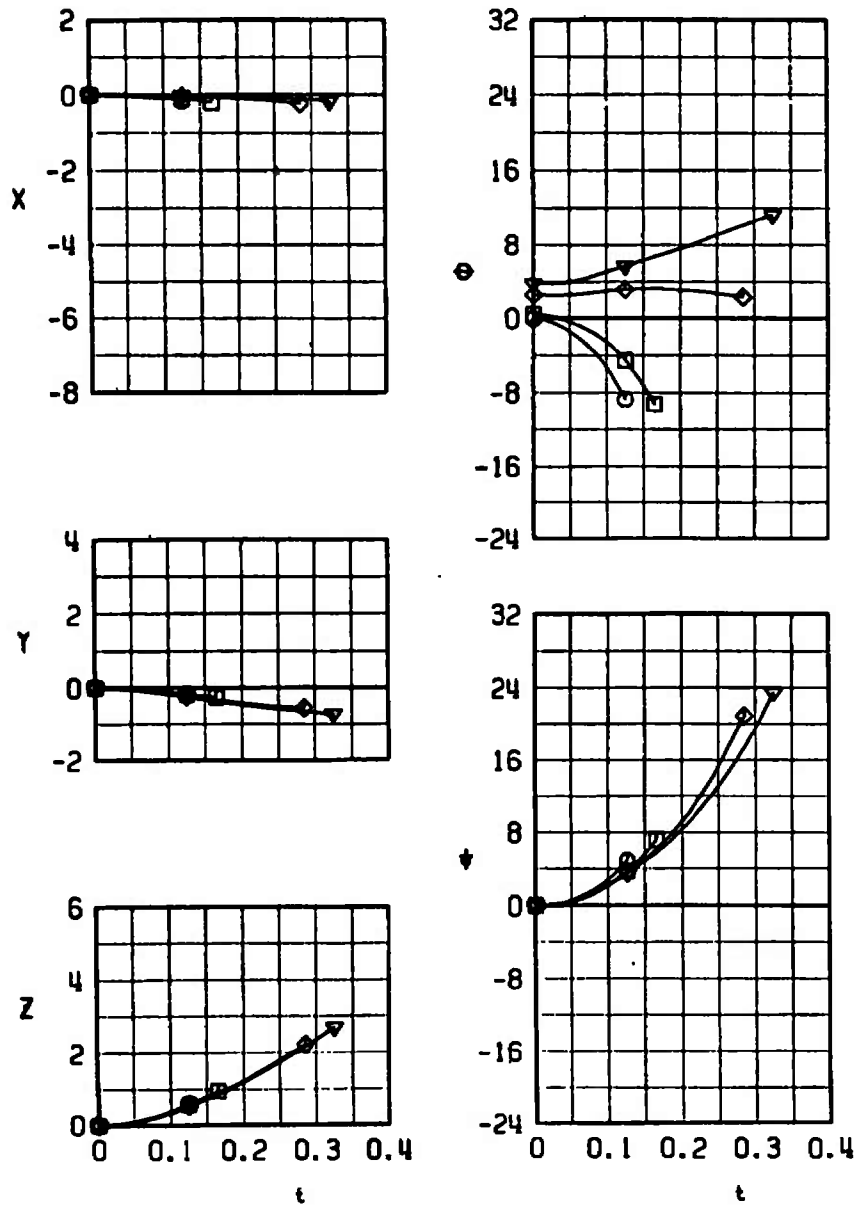
i. MER, Configuration 9H, MER Aft  
Fig. 13 Concluded



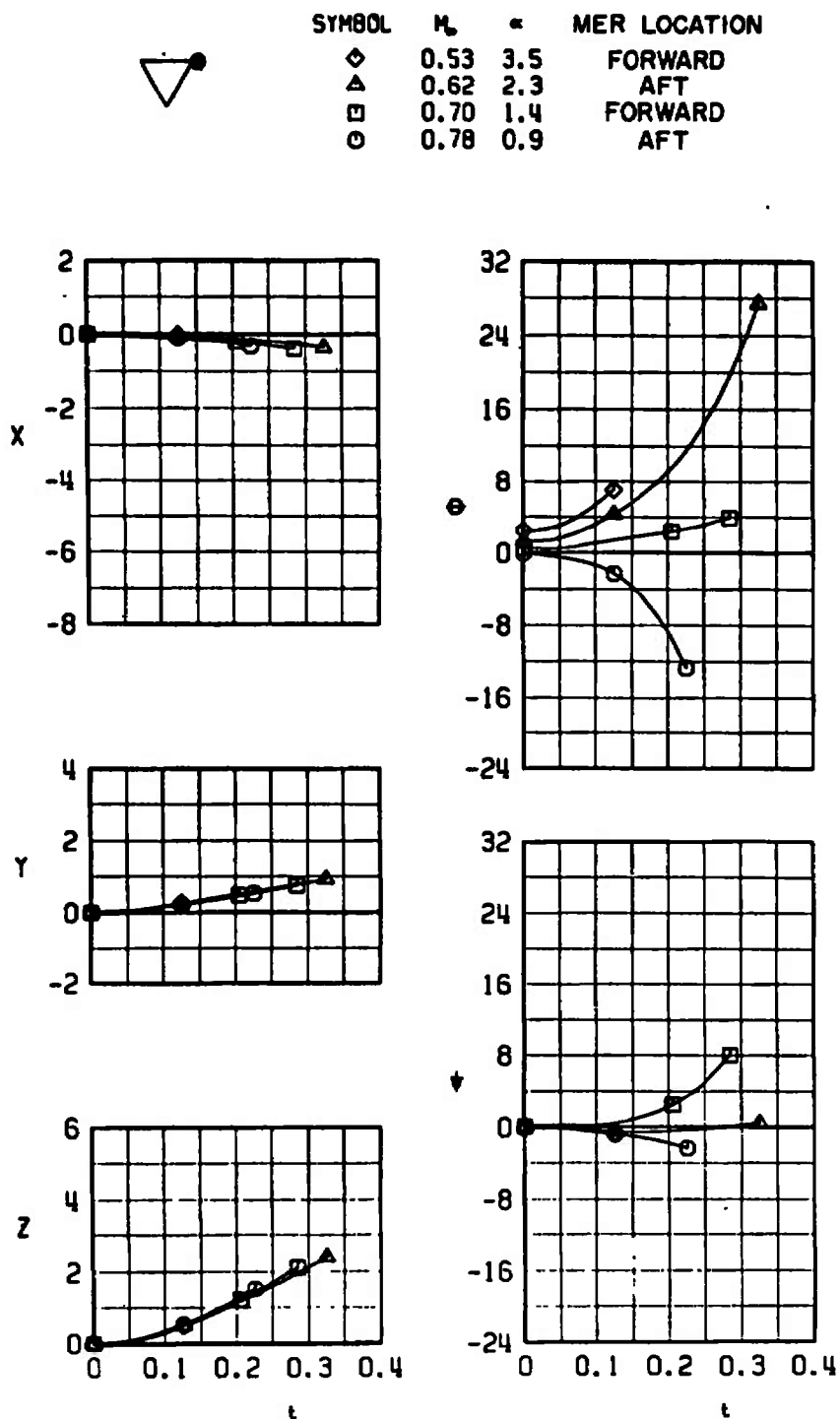
a. TER, Configuration 1L, MER Forward

Fig. 14 Effects of Mach Number on the Separation Characteristics of the LAU-69/A (Full with the Light Warhead) from the Inboard TER and Centerline MER

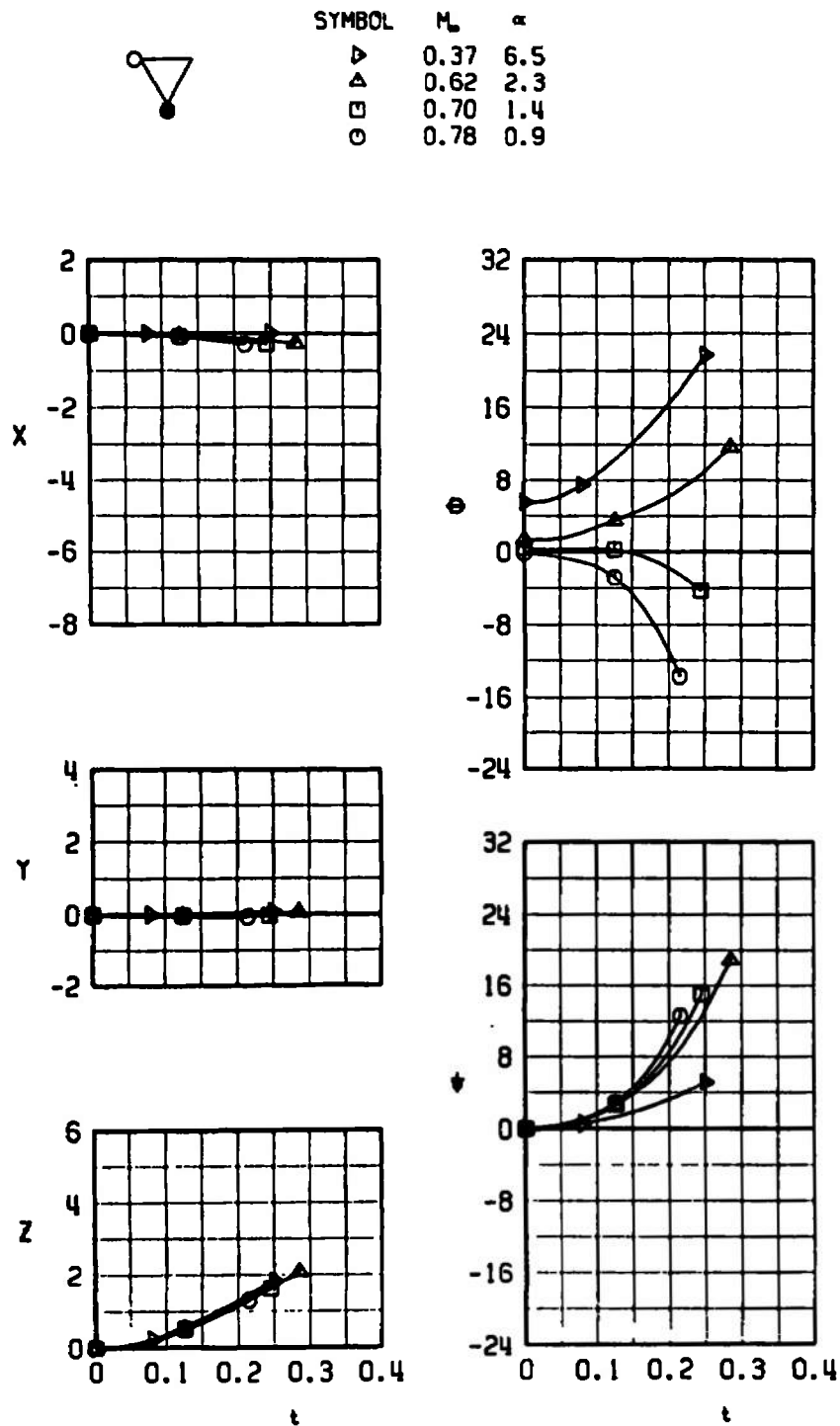
SYMBOL	$M_\infty$	$\alpha$
	0.45	4.8
	0.53	3.5
	0.70	1.4
	0.78	0.9



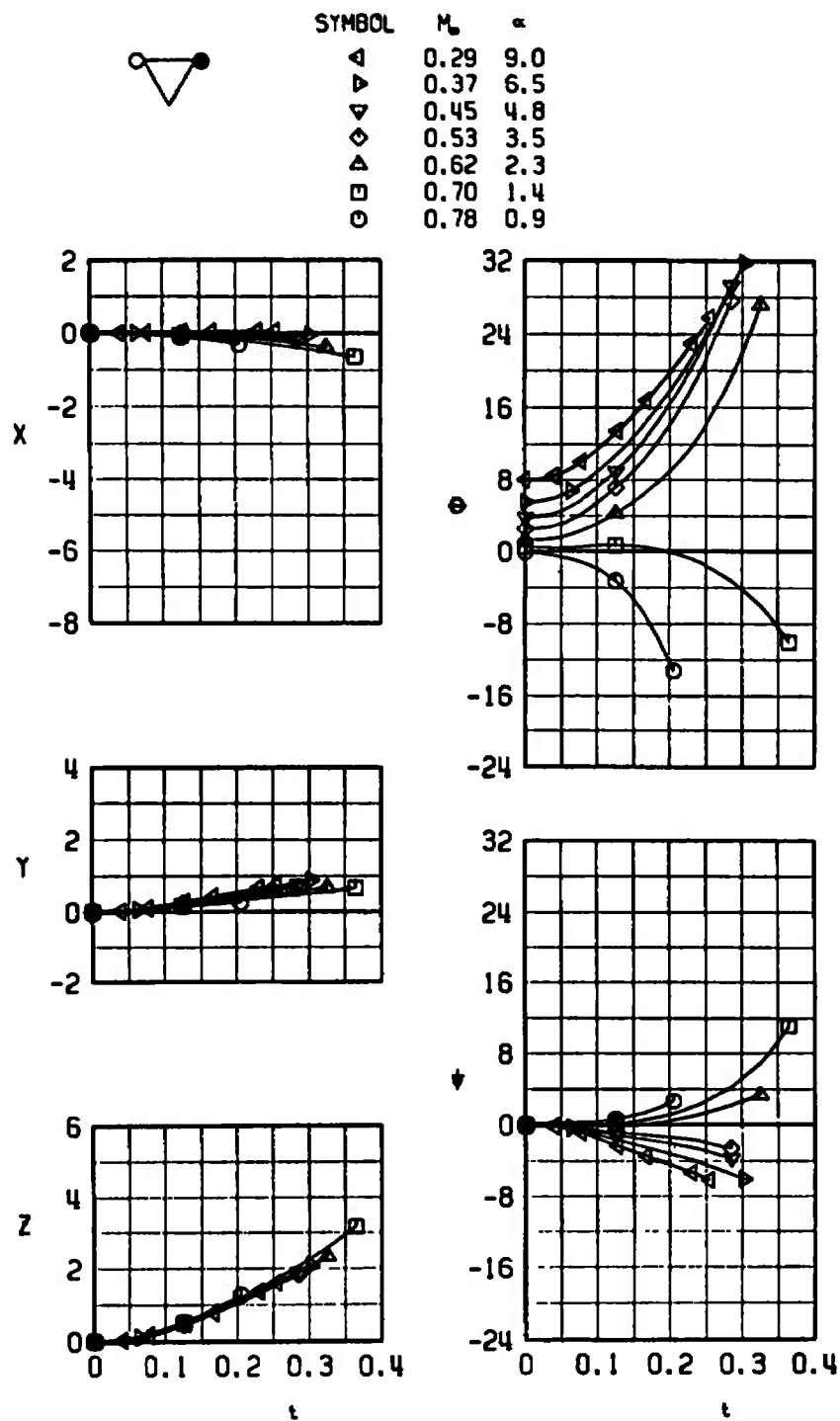
b. TER, Configuration 2L, MER Aft  
Fig. 14 Continued



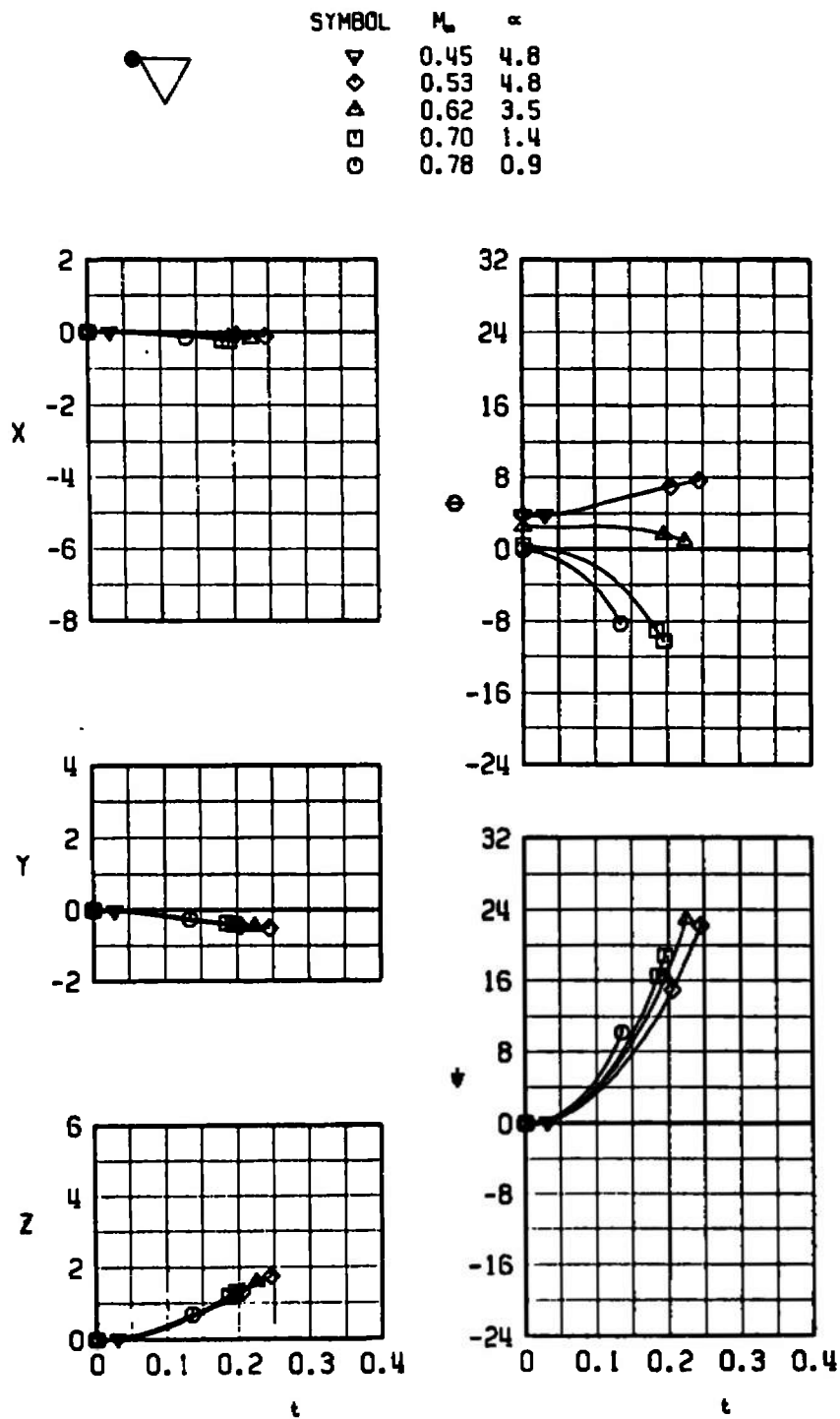
c. TER, Configuration 3L  
Fig. 14 Continued



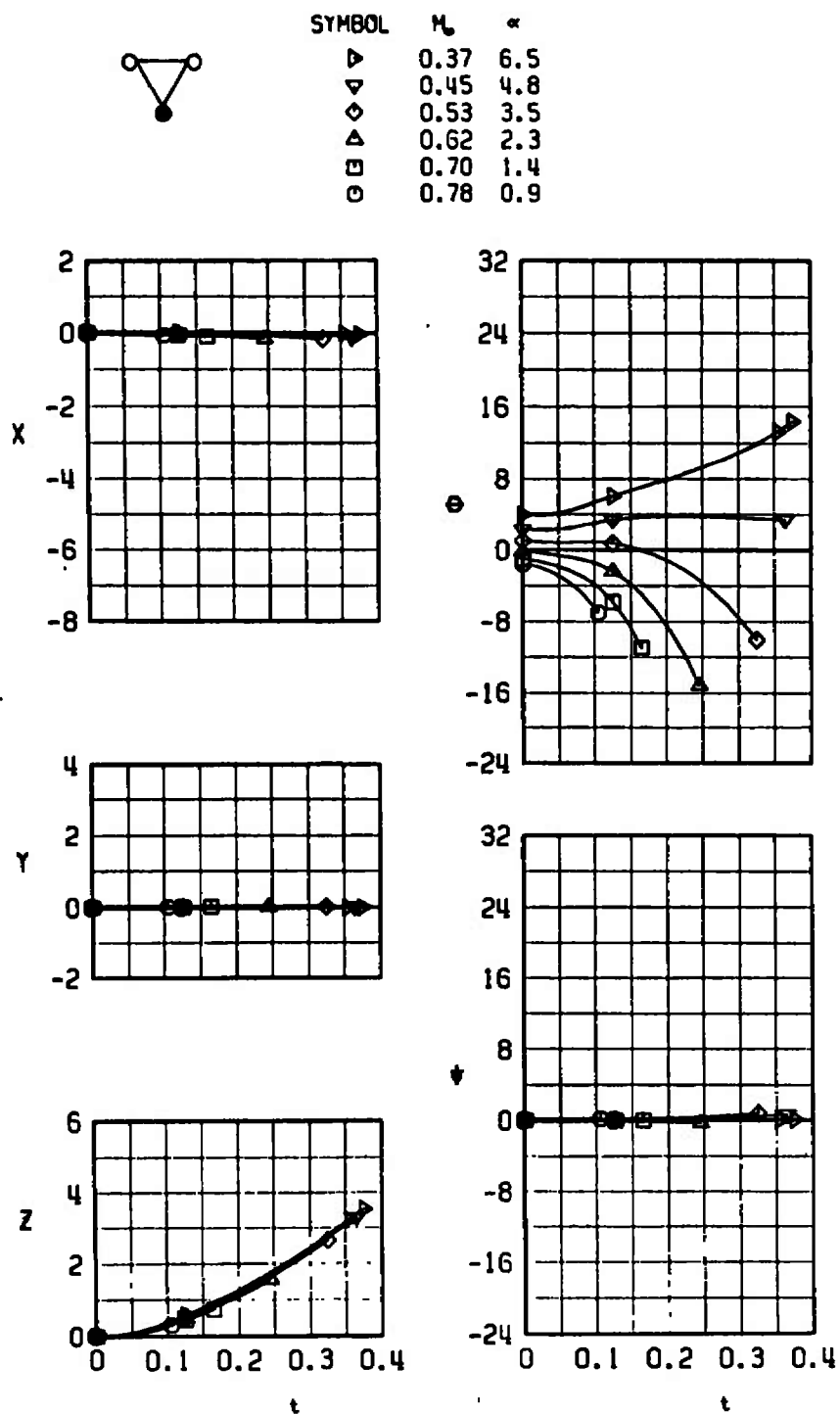
d. TER, Configuration 4L, MER Forward  
Fig. 14 Continued



e. TER, Configuration 5L, MER Forward  
Fig. 14 Continued

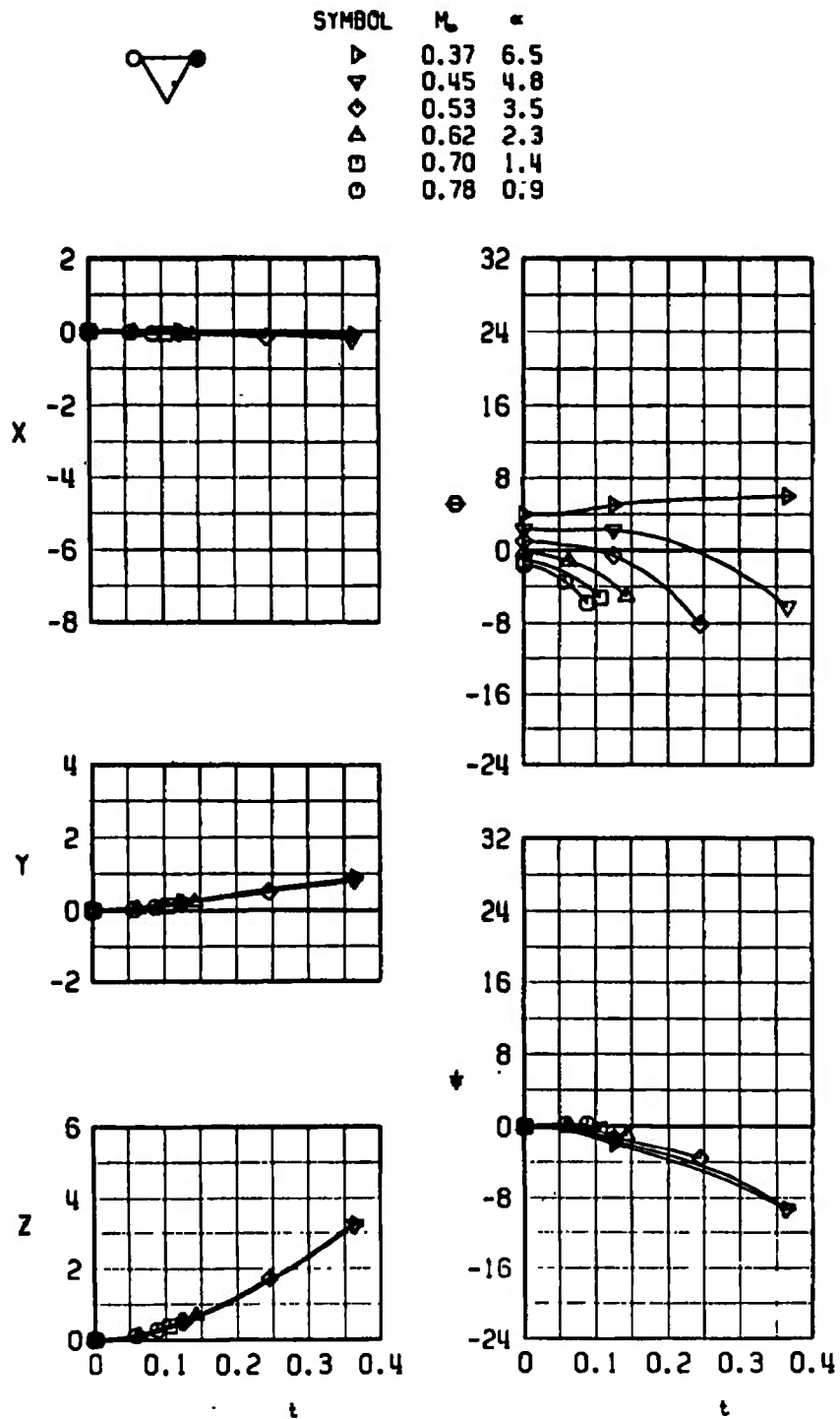


f. TER, Configuration 6L, MER Aft  
Fig. 14 Continued

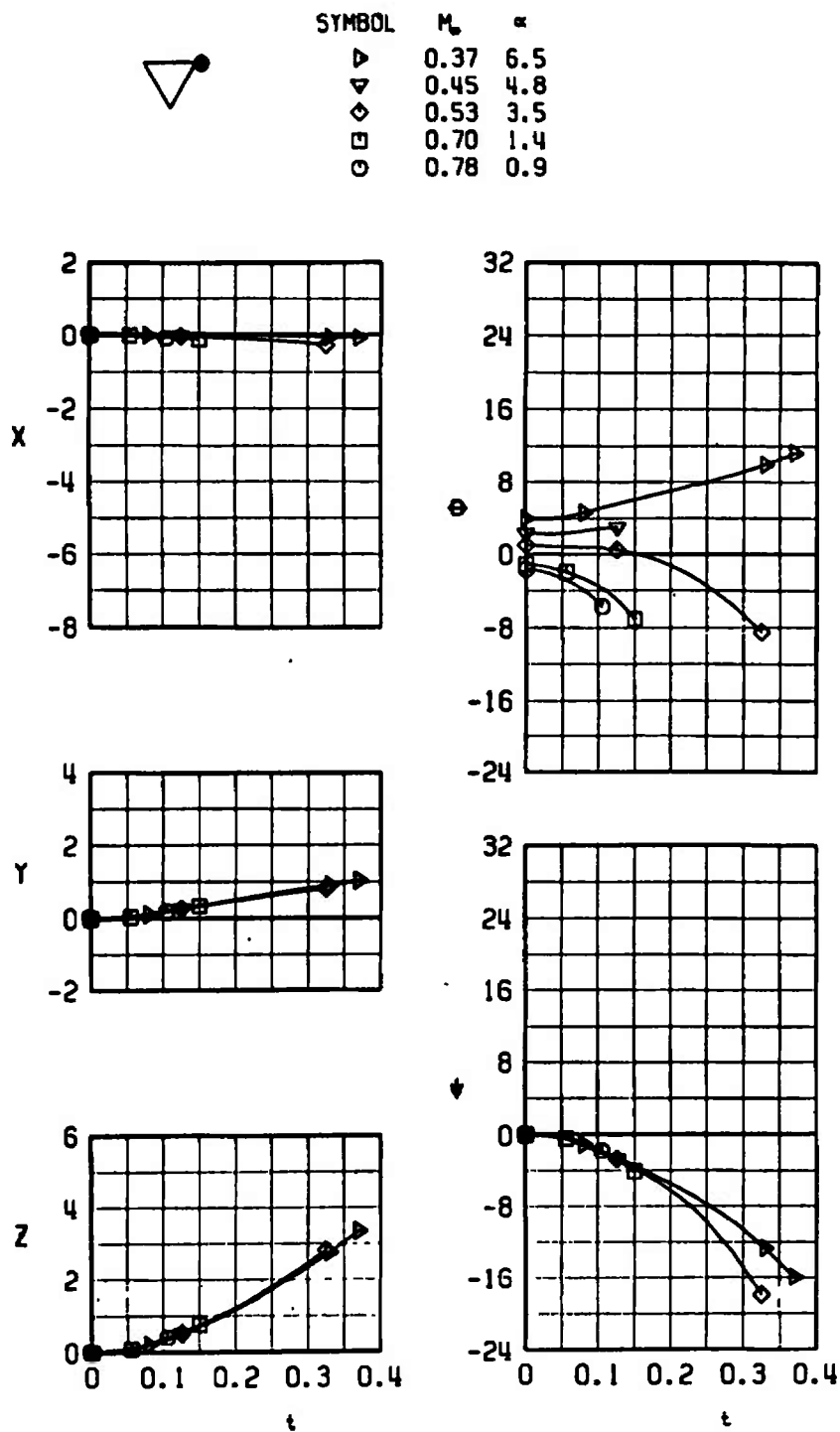


g. MER, Configuration 7L, MER Aft  
Fig. 14 Continued

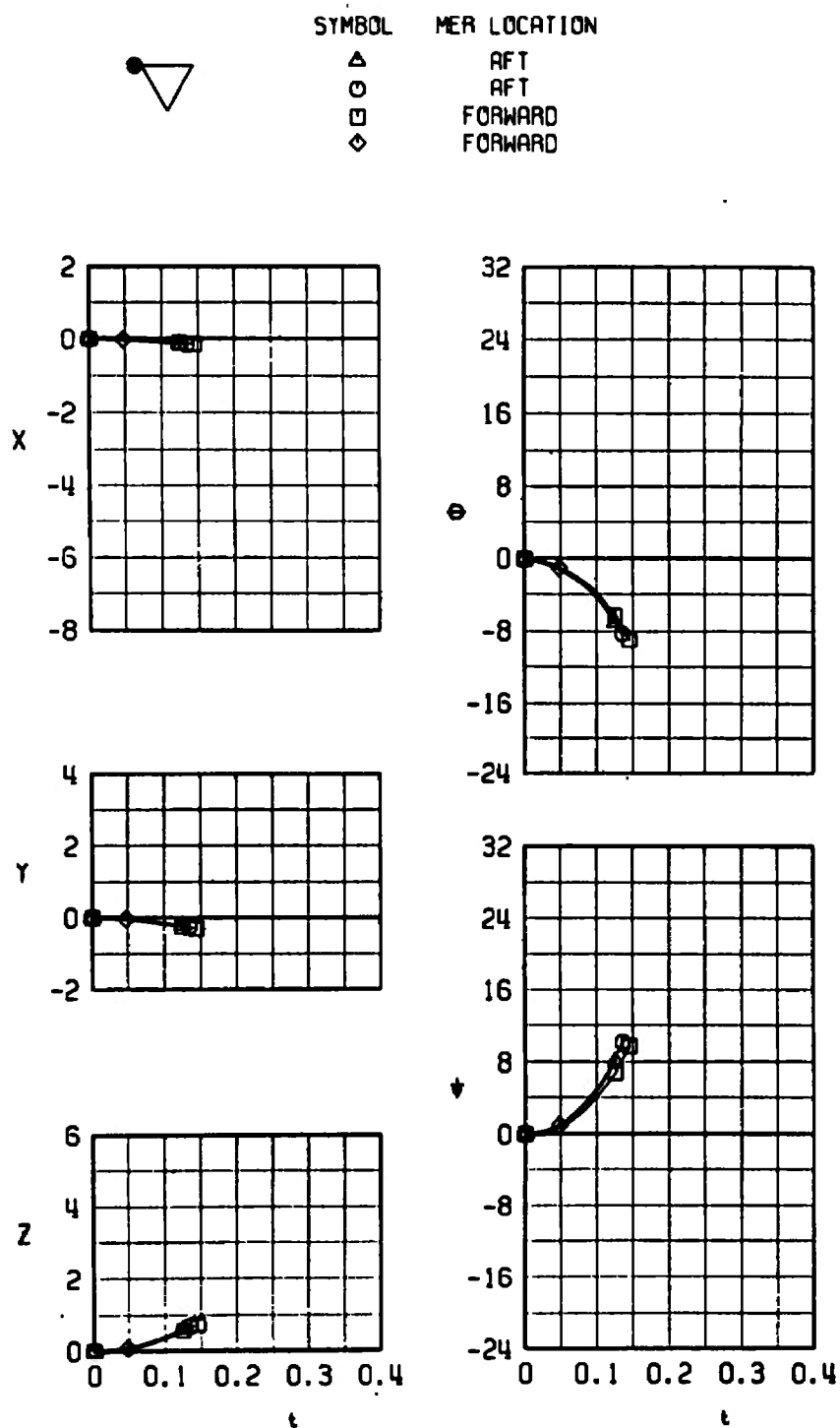




h. MER, Configuration 8L, MER Aft  
Fig. 14 Continued

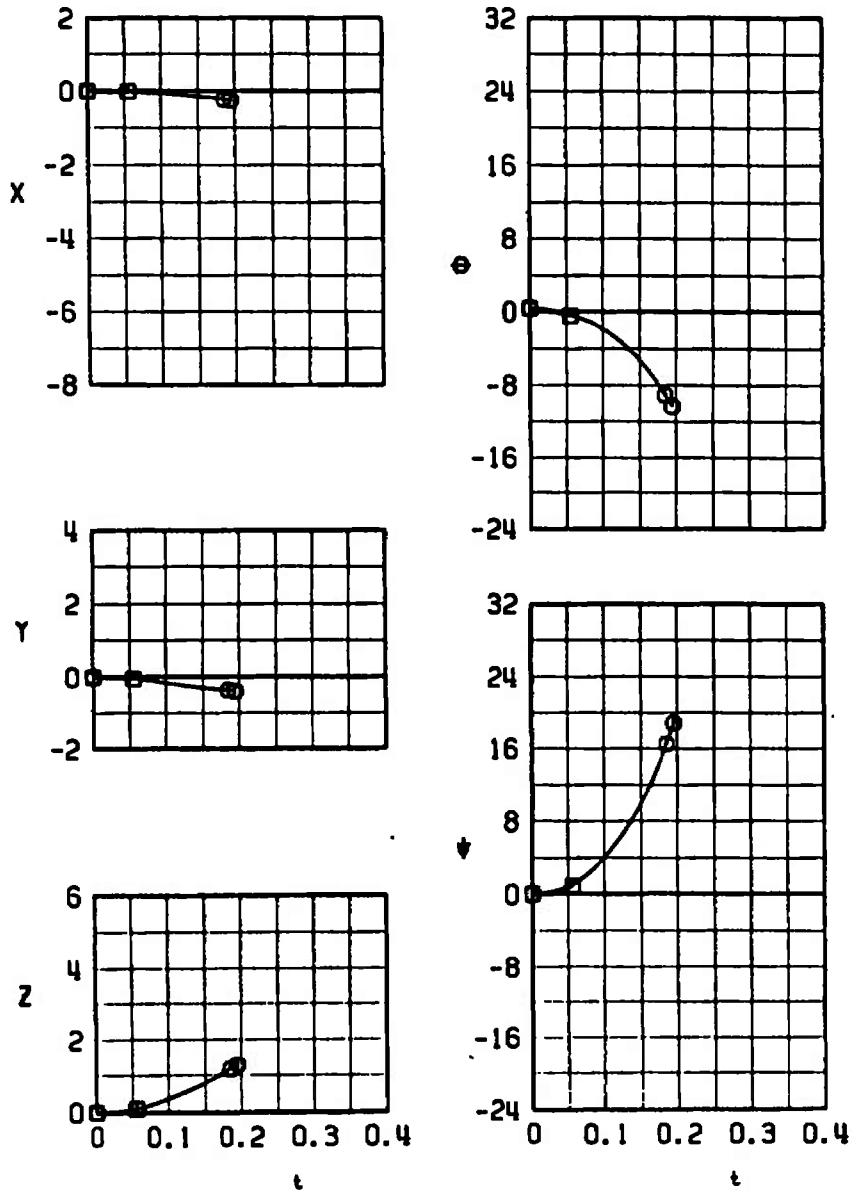
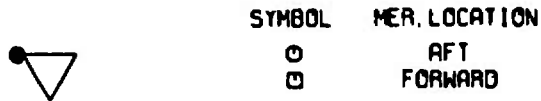


i. MER, Configuration 9L, MER Aft  
Fig. 14 Concluded

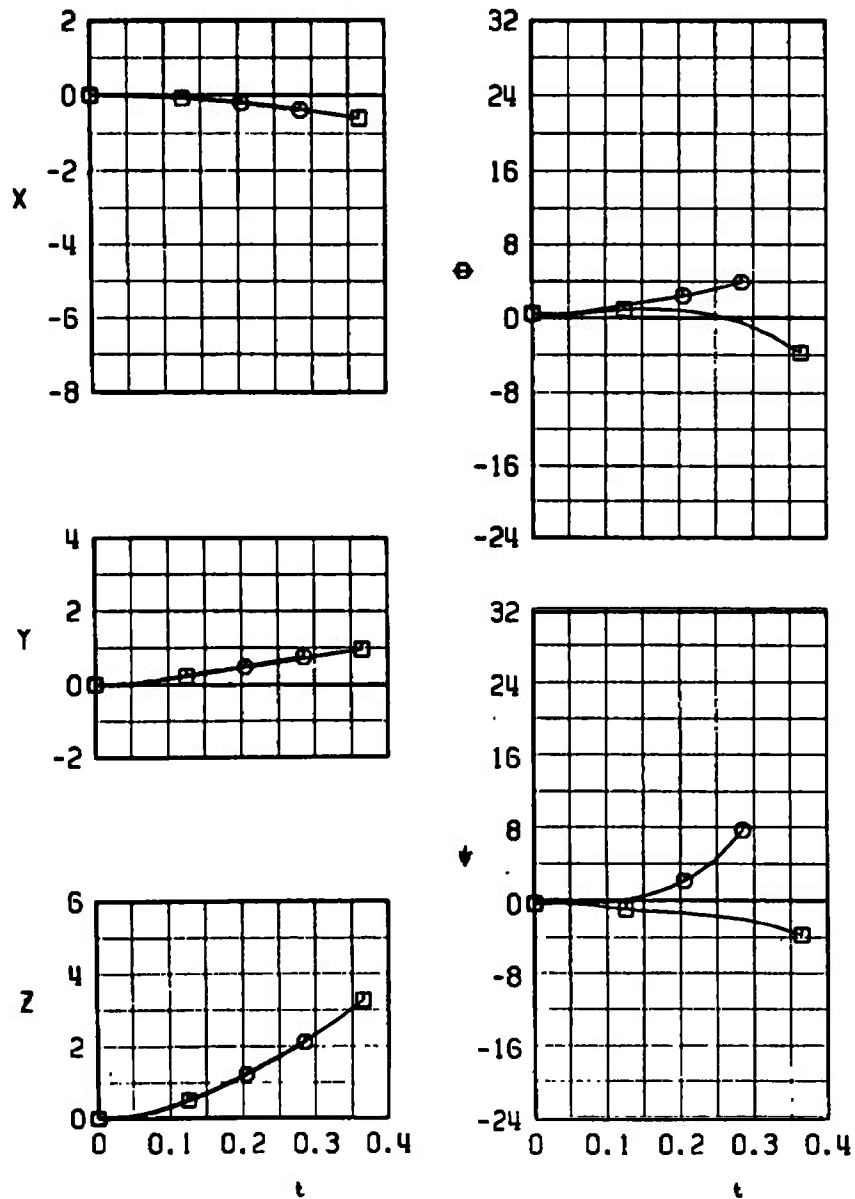
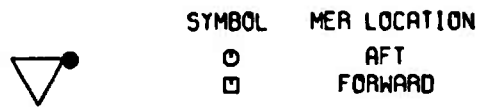


a.  $M_\infty = 0.78$ , Configuration 6L,  $\alpha = 0.9$

Fig. 15 Comparison of Trajectories of the Full LAU-69/A from the TER with MER in Forward and Aft Locations



b.  $M_\infty = 0.70$ , Configuration 6L,  $\alpha = 0.9$   
 Fig. 15 Continued



c.  $M_\infty = 0.70$ , Configuration 3L,  $\alpha = 1.4$   
Fig. 15 Concluded

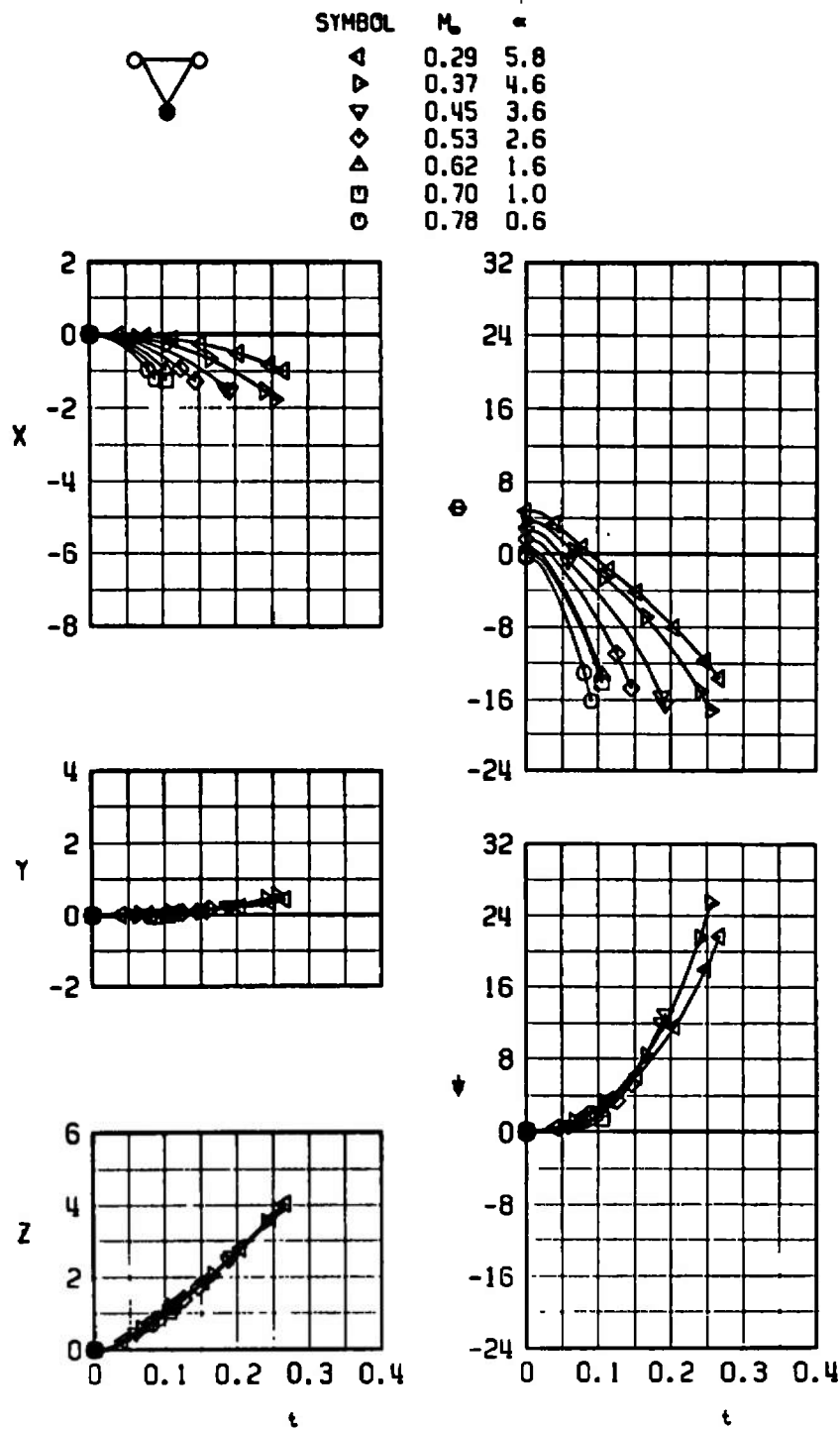
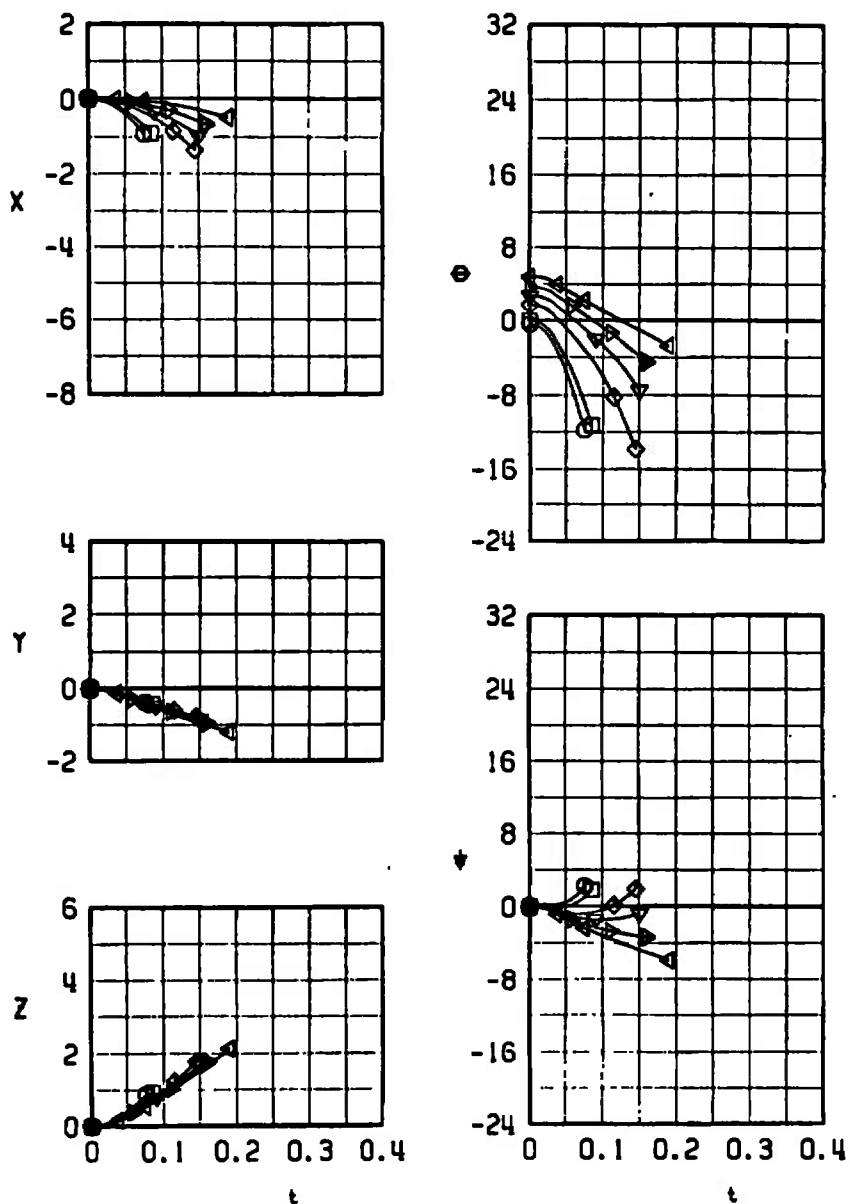
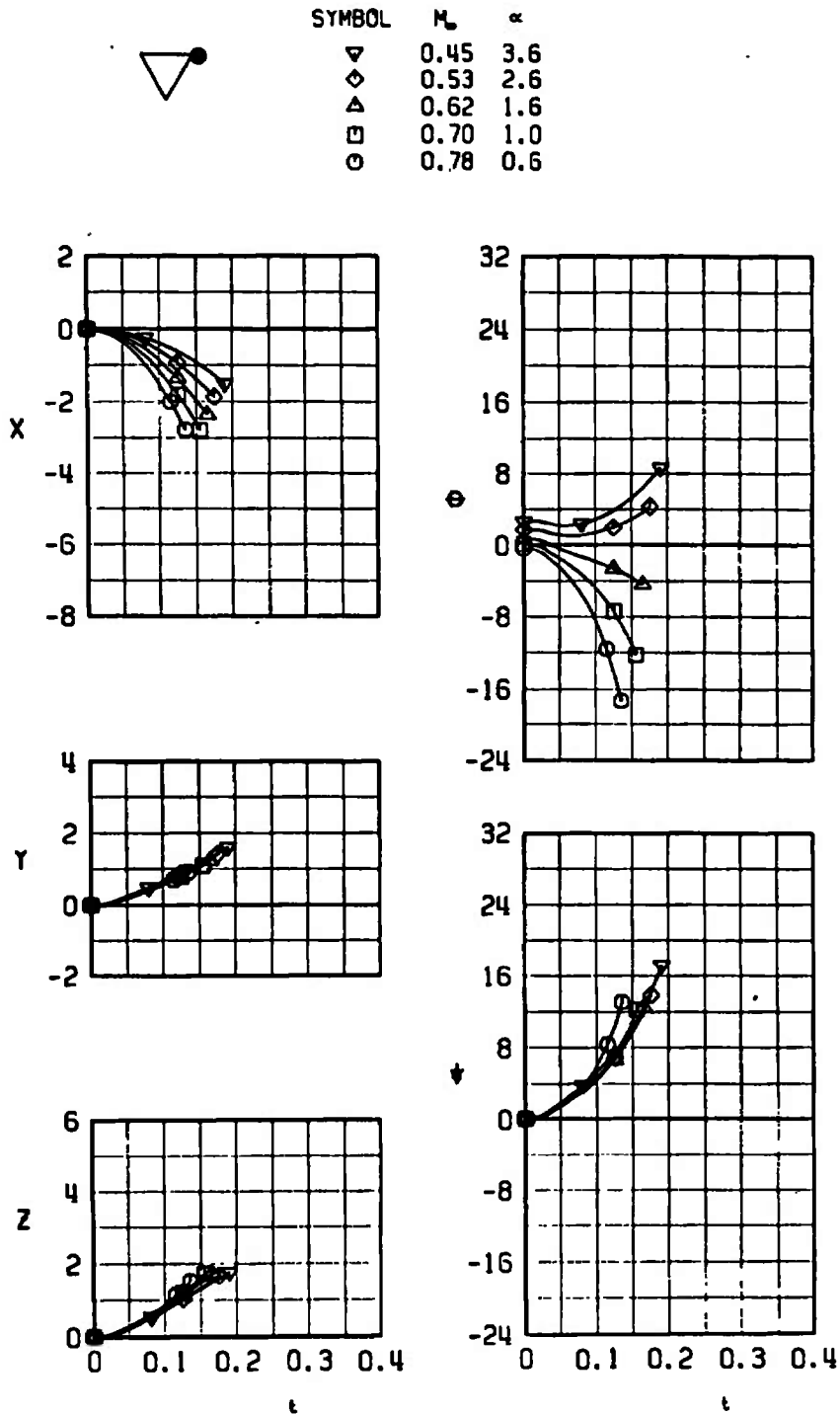


Fig. 16 Effect of Mach Number on the Separation Characteristics of the LAU-69/A (Empty) from the Inboard TER and Centerline MER

SYMBOL	$M_\infty$	$\alpha$
$\triangleleft$	0.29	5.8
$\triangleright$	0.37	4.6
$\nabla$	0.45	3.6
$\diamond$	0.53	2.6
$\square$	0.70	1.0
$\circ$	0.78	0.6



b. TER, Configuration 2E, MER Aft  
Fig. 16 Continued

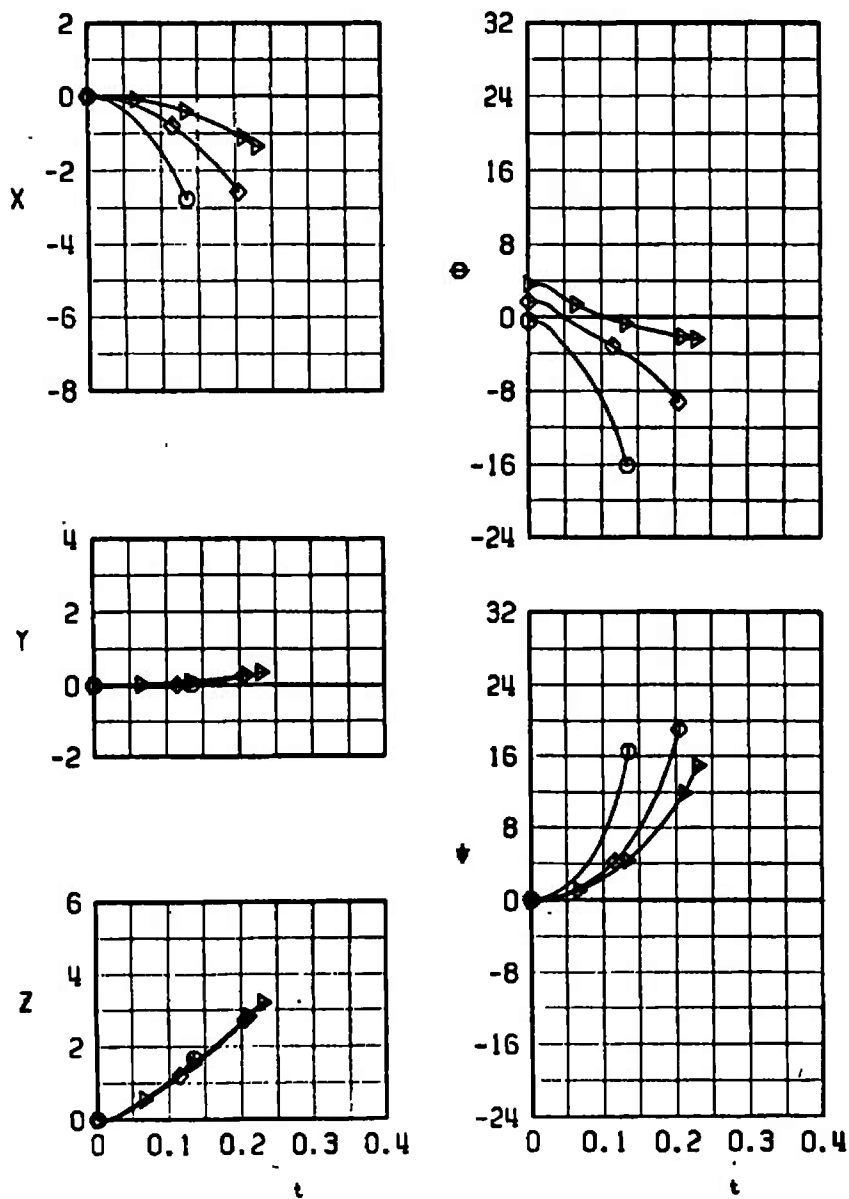


c. TER, Configuration 3E, MER Aft  
Fig. 16 Continued





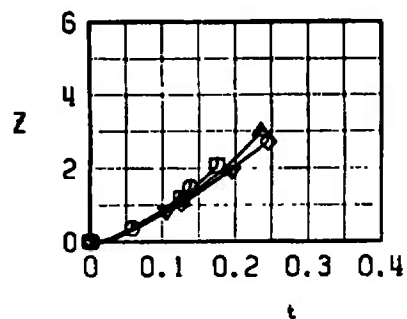
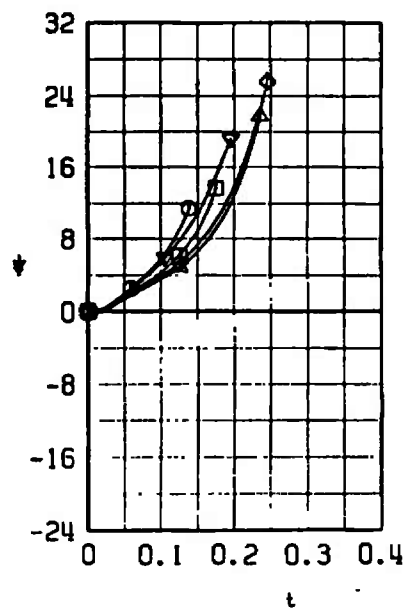
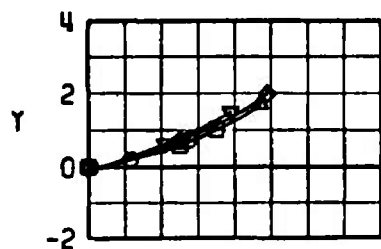
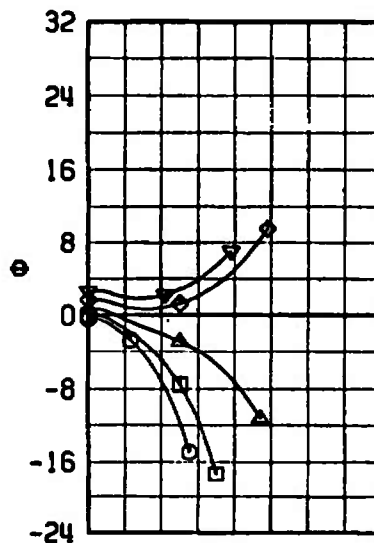
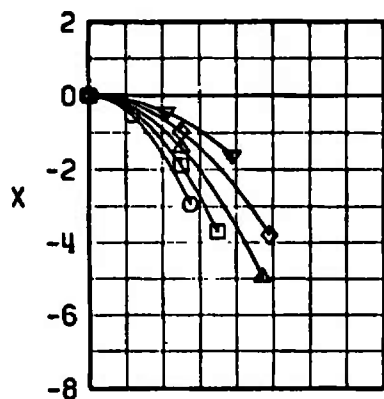
SYMBOL	$M_\infty$	$\alpha$
$\blacktriangleright$	0.37	4.6
$\diamond$	0.53	2.6
$\circ$	0.78	0.6



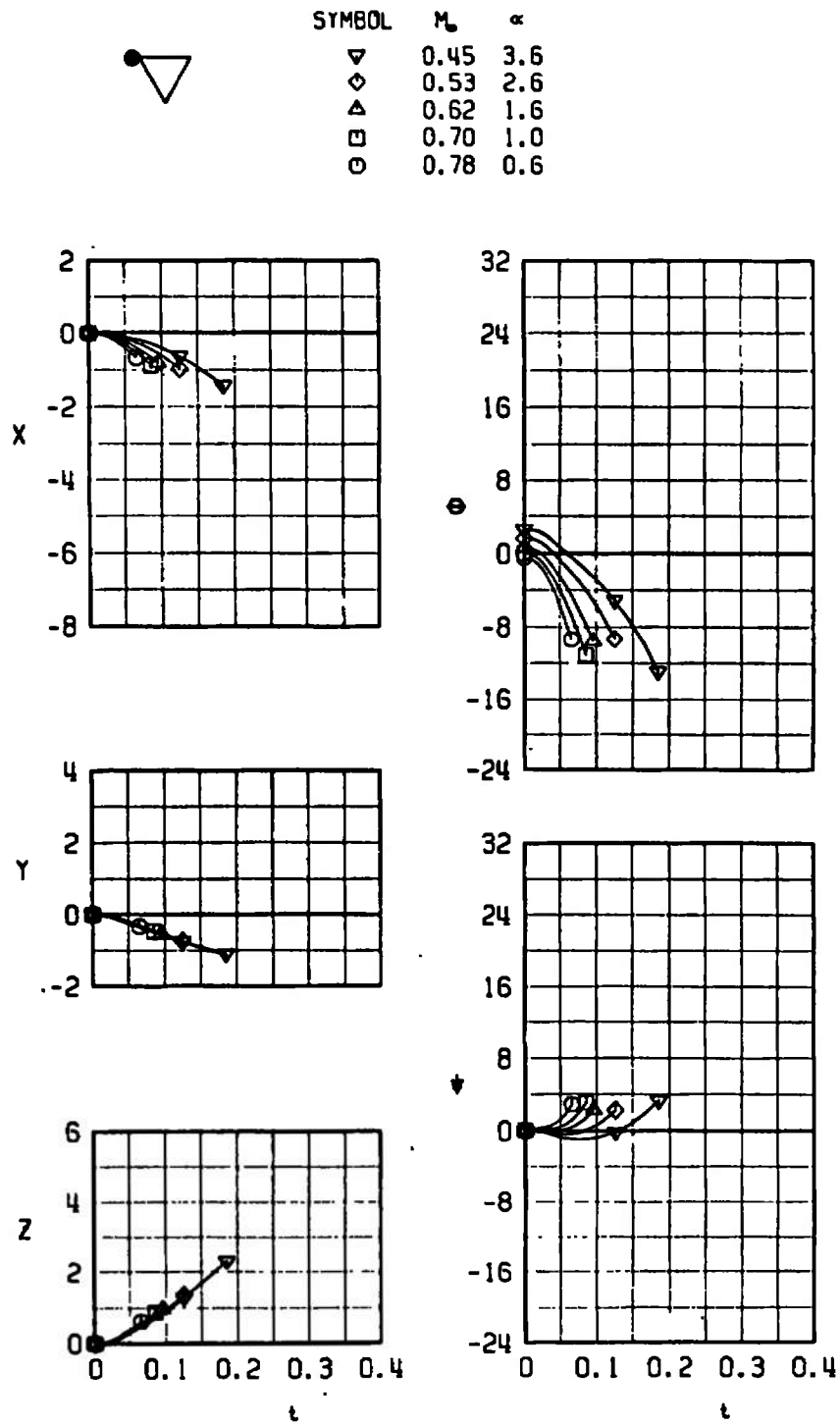
d. TER, Configuration 4E, MER Aft  
Fig. 16 Continued



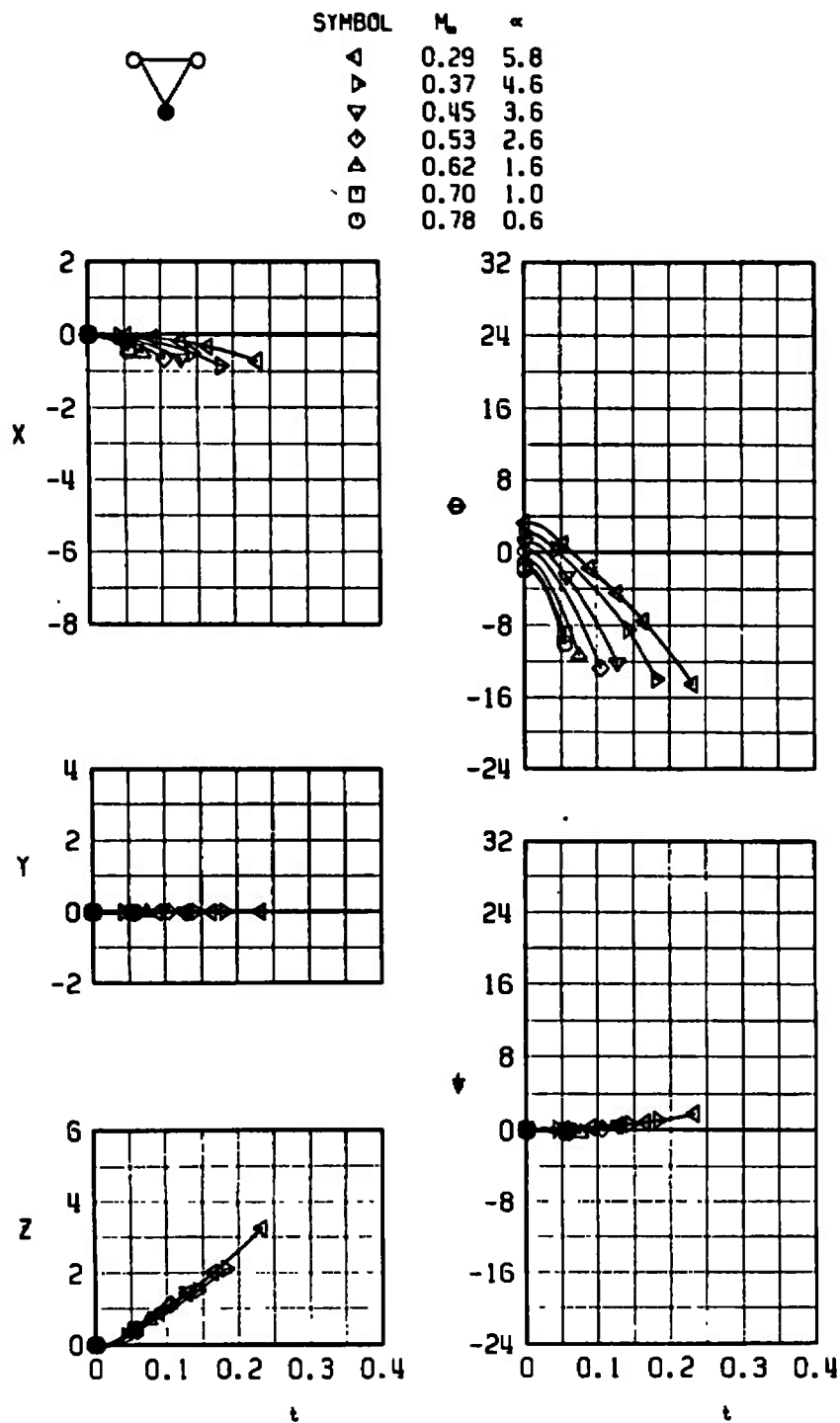
SYMBOL	$M_\infty$	$\alpha$
$\nabla$	0.45	3.6
$\diamond$	0.53	2.6
$\triangle$	0.62	1.6
$\square$	0.70	1.0
$\circ$	0.78	0.6



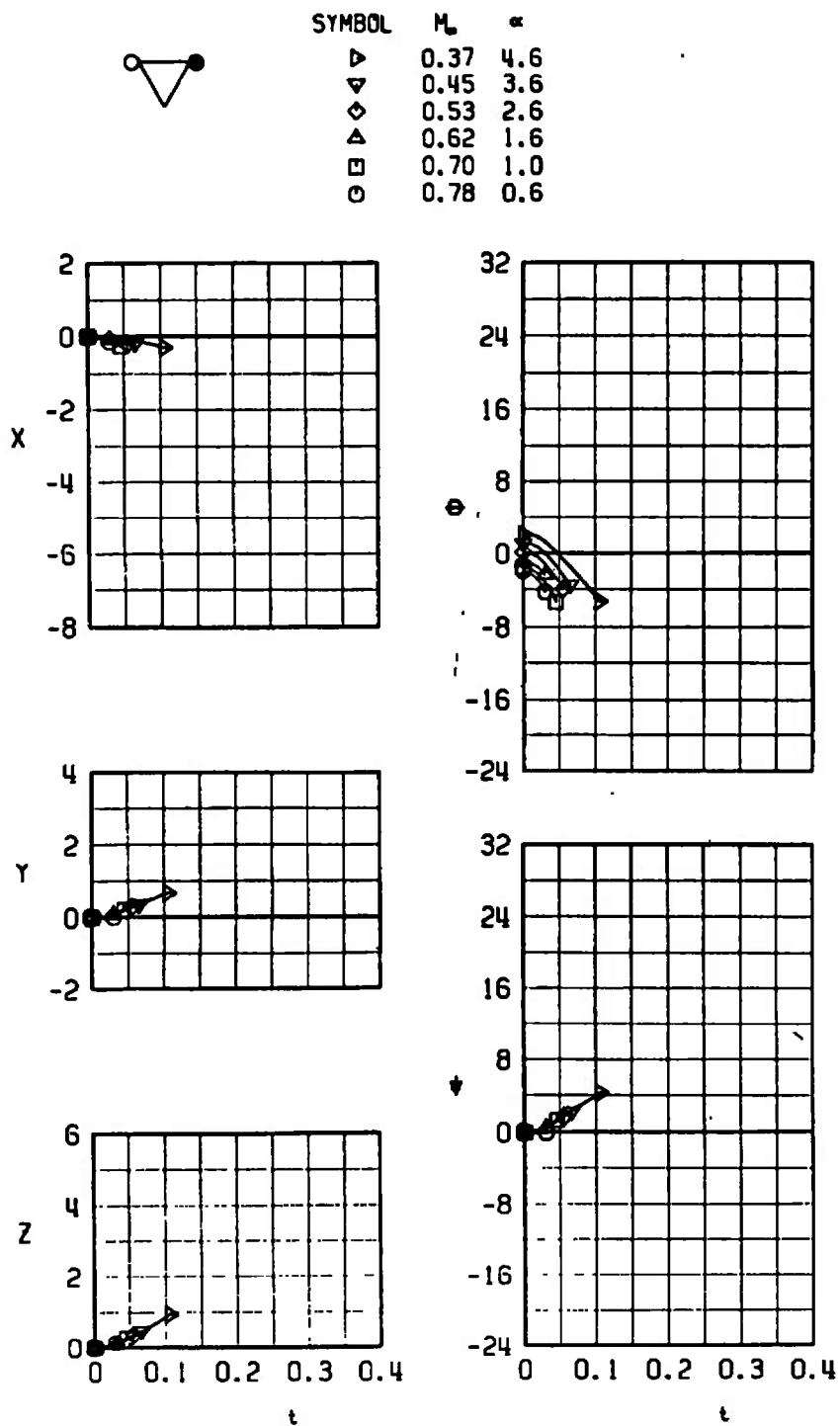
e. TER, Configuration 5E, MER Aft  
Fig. 16 Continued



f. TER, Configuration 6E, MER Aft  
Fig. 16 Continued



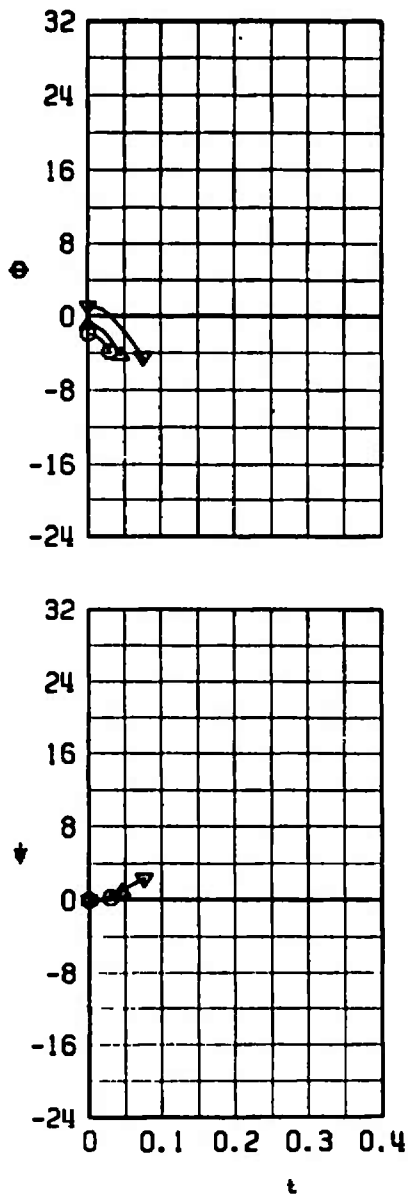
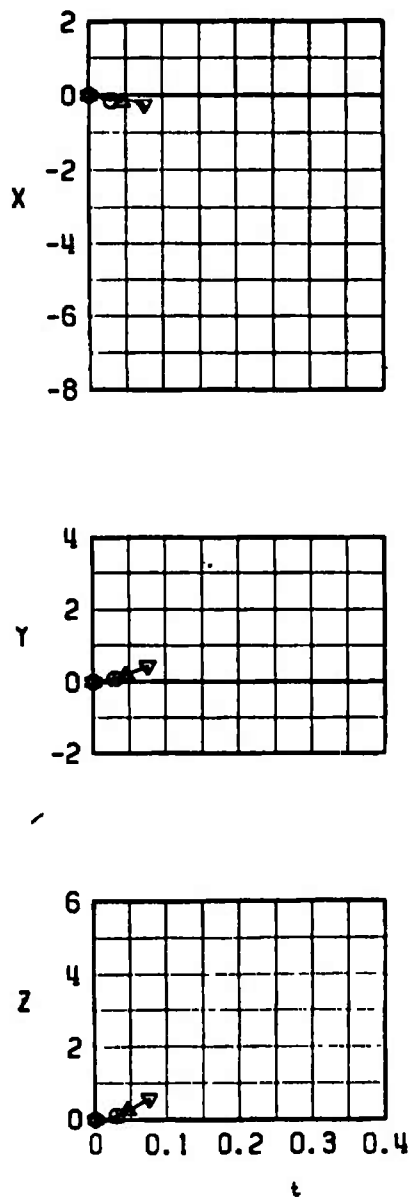
g. MER, Configuration 7E, MER Aft  
Fig. 16 Continued



h. MER, Configuration 8E, MER Aft  
Fig. 16 Continued



SYMBOL	$M_\infty$	$\alpha$
$\nabla$	0.45	3.6
$\triangle$	0.62	1.6
$\circ$	0.78	0.6



i. MER, Configuration 9E, MER Aft  
Fig. 16 Concluded

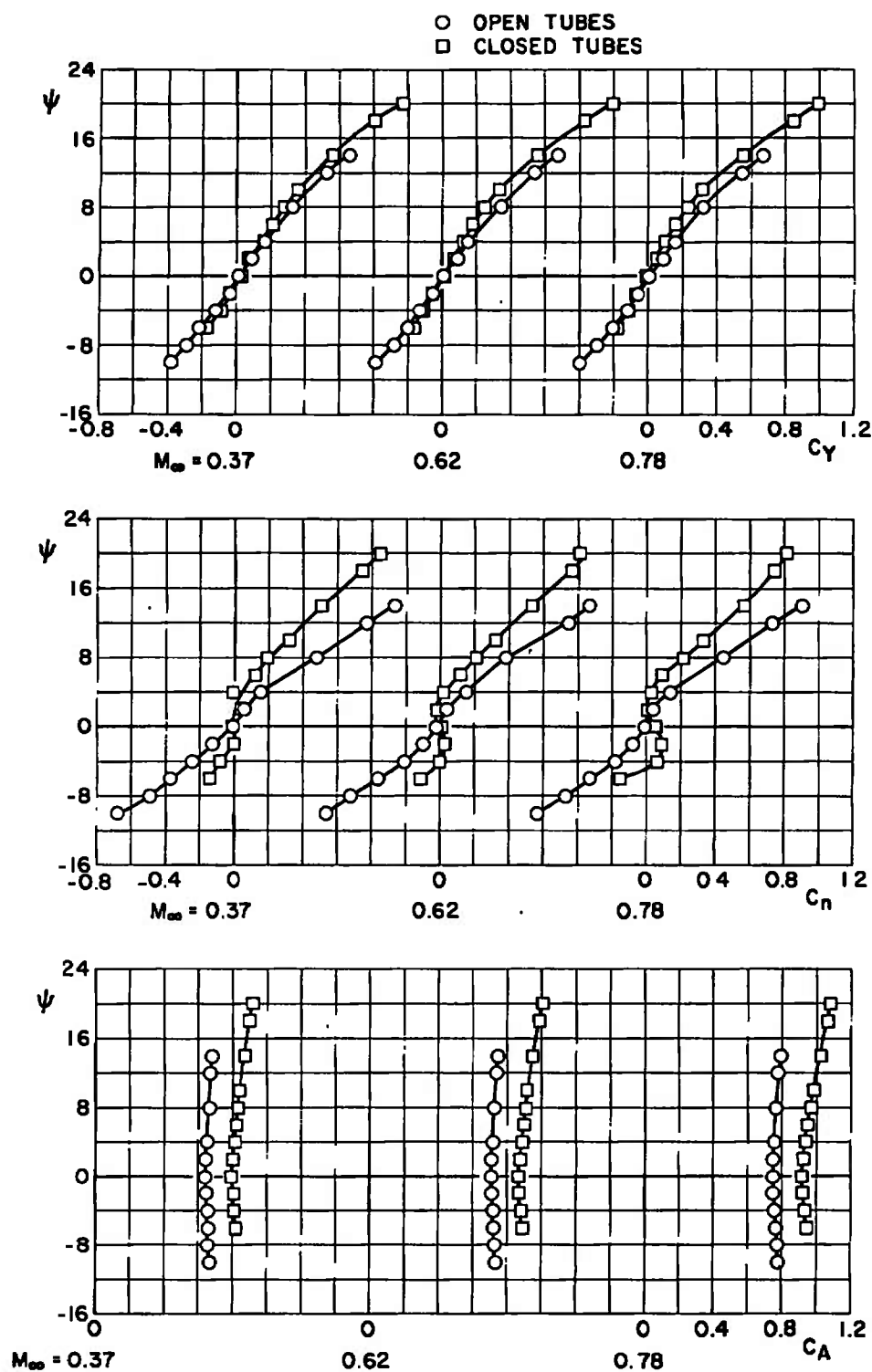
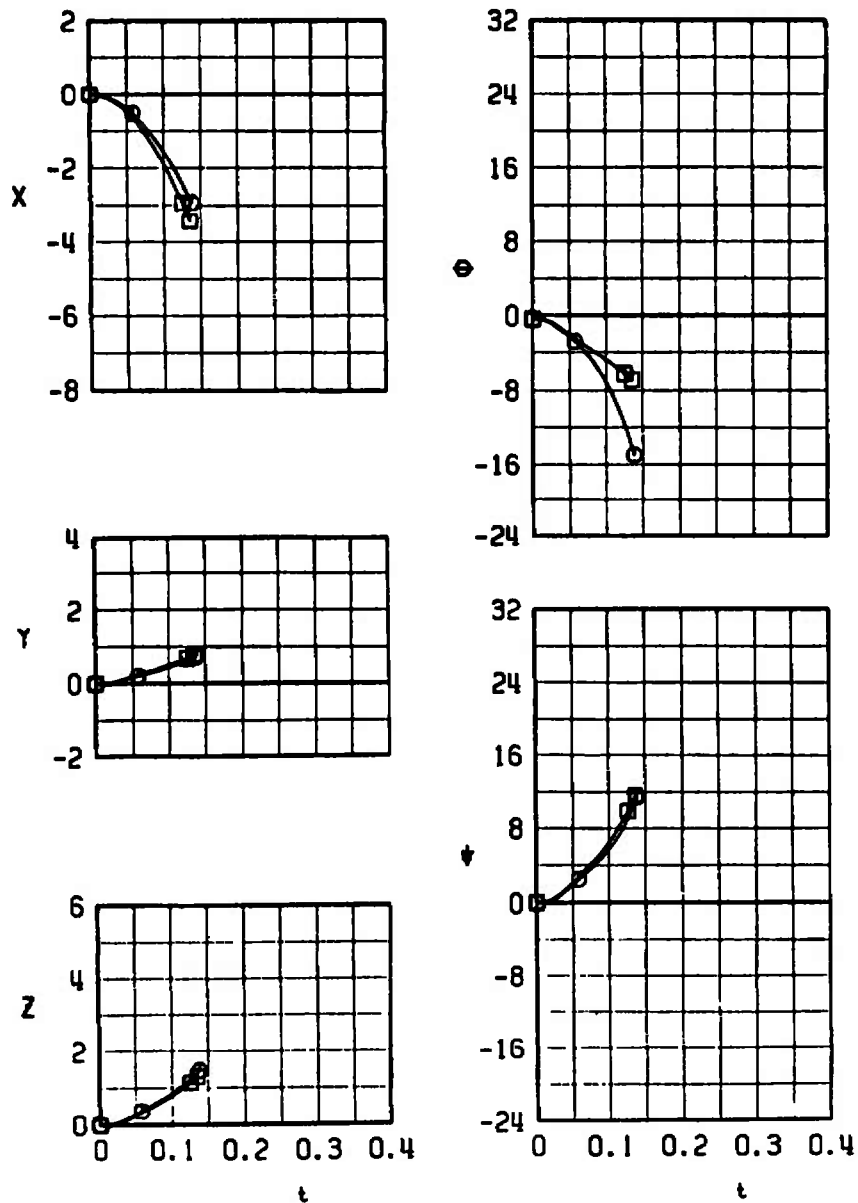


Fig. 17 Free-Stream Static Stability and Axial-Force Data Comparing Open and Closed Tubes, LAU-69/A, Empty, for  $M_\infty = 0.37, 0.62$ , and  $0.78$



○ OPEN TUBES  
□ CLOSED TUBES



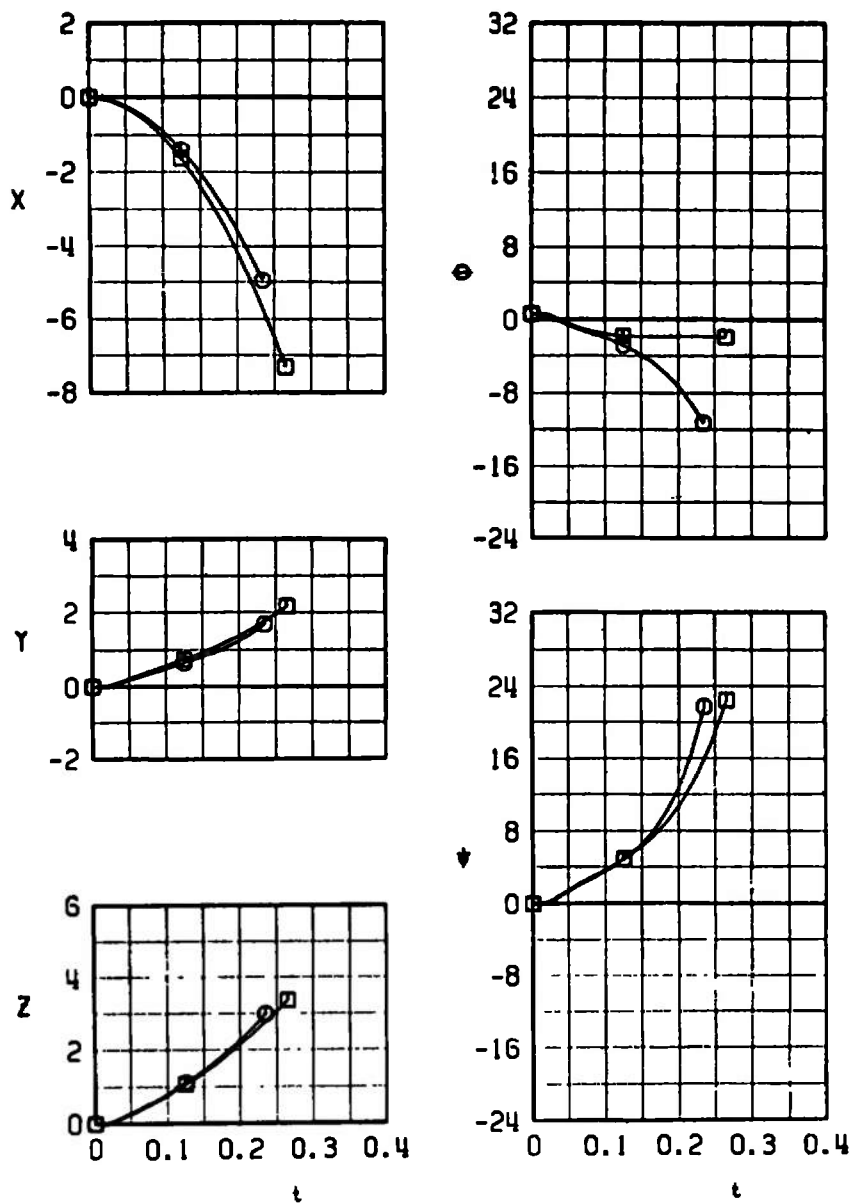
a.  $M_\infty = 0.62$ ,  $\alpha = 1.0$

Fig. 18 Comparisons of Trajectories Obtained with Open and Closed Tubes, LAU-69/A, Empty, Configuration 5E, MER Aft





○ OPEN TUBES  
□ CLOSED TUBES



b.  $M_\infty = 0.78$ ,  $\alpha = 0.6$

Fig. 18 Concluded

TABLE I  
SUMMARY OF TEST CONDITIONS

<u><math>M_{\infty}</math></u>	<u><math>q_{\infty}</math>, psf</u>
0.29	185
0.37	294
0.45	417
0.53	500
0.62	500
0.70	500
0.78	500

TABLE II  
FULL-SCALE STORE PARAMETERS USED IN TRAJECTORY CALCULATIONS

PARAMETER	LAU 69/A (Full Light)	LAU 69/A Full (Heavy)	LAU 69/A Empty
Pitch-Damping Derivative $C_{mq}$ , per radian	-27.0	-27.0	-45.0
Yaw-Damping Derivative $C_{nr}$ , per radian	-27.0	-27.0	-45.0
Mass, $\bar{m}$ , slugs	20.10	23.30	2.79
Center of Gravity with Respect to Store Nose, $X_{cg}$ , ft	3.373	3.077	2.598
Store Reference Width, $b$ , ft	1.308	1.308	1.308
Ejector Piston Location Relative to Store cg, $X_L$ , ft	-0.341	-0.637	0.318
Moment of Inertia, $I_{xx}$ , slug-ft <sup>2</sup>	3.648	4.21	0.805
Moment of Inertia, $I_{yy}$ , slug-ft <sup>2</sup>	38.06	51.559	7.571
Moment of Inertia, $I_{zz}$ , slug-ft <sup>2</sup>	37.892	51.443	7.337

NOTE: "Light" and "Heavy" indicate light and heavy war heads.

**TABLE III  
LOAD CONFIGURATIONS**

Configuration	Centerline Pylon with MER	Inboard Pylon with TER	Outboard Pylon
1L, 1H, 1E	LAU-69/A Dummy Sta 2, 6	LAU-69/A Launch Sta 1 LAU-69/A Dummy Sta 2, 3	370-Gal Fuel Tank
2L, 2H, 2E		LAU-69/A Launch Sta 2 LAU-69/A Dummy Sta 3	
3L, 3H, 3E		LAU-69/A Launch Sta 3	
5L, 5H, 5E		LAU-69/A Launch Sta 3 LAU-69/A Dummy Sta 2	
6L, 6H, 6E		LAU-69/A Launch Sta 2	
4L, 4H, 4E		LAU-69/A Launch Sta 1 LAU-69/A Dummy Sta 2	
7L, 7H, 7E	LAU-69/A Launch Sta 2 LAU-69/A Dummy Sta 4, 6	Empty TER	
8L, 8H, 8E	LAU-69/A Launch Sta 6 LAU-69/A Dummy Sta 4		
9L, 9H, 9E	LAU-69/A Launch Sta 6		

**NOTE:** Suffixes L and H refer to light or heavy warhead and E indicates an empty launcher.

UNCLASSIFIED

Security Classification

## DOCUMENT CONTROL DATA - R &amp; D

(Security classification of title, body of abstract and indexing annotation must be entered when the overall report is classified)

1. ORIGINATING ACTIVITY (Corporate author)		2a. REPORT SECURITY CLASSIFICATION	
Arnold Engineering Development Center Arnold Air Force Station, Tennessee		UNCLASSIFIED	
		2b. GROUP	
		N/A	
3. REPORT TITLE			
SEPARATION CHARACTERISTICS OF THE LAU-69/A ROCKET LAUNCHER FROM THE F-4C AIRCRAFT AT MACH NUMBERS FROM 0.29 TO 0.78			
4. DESCRIPTIVE NOTES (Type of report and inclusive dates)			
Final Report - August 2 to 8, 1971			
5. AUTHOR(S) (First name, middle initial, last name)			
A. C. Mansfield, ARO, Inc.			
6. REPORT DATE		7a. TOTAL NO. OF PAGES	7b. NO. OF REFS
October 1971		67	2
8a. CONTRACT OR GRANT NO.		9a. ORIGINATOR'S REPORT NUMBER(S)	
b. PROJECT NO. 2592		AEDC-TR-71-228	
c. Program Element 64602F		AFATL-TR-71-134	
d. Task 04		9b. OTHER REPORT NO(S) (Any other numbers that may be assigned this report)	
		ARO-PWT-TR-71-178	
10. DISTRIBUTION STATEMENT			
Distribution limited to U.S. Government agencies only; this report contains information on test and evaluation of military hardware; October 1971; other requests for this document must be referred to Air Force Armament Laboratory (DLGC), Eglin AFB, Florida 32542.			
11. SUPPLEMENTARY NOTES		12. SPONSORING MILITARY ACTIVITY	
Available in DDC		AFATL (DLGC) Eglin AFB, Florida 32542	
13. ABSTRACT			
<p>A wind-tunnel test was conducted using 0.05-scale models to study the separation characteristics of the LAU-69/A rocket launcher, both full and empty, from the F-4C aircraft. The separation trajectories were initiated from the right-wing inboard pylon station utilizing the Triple Ejection Rack and from the centerline pylon utilizing the Multiple Ejection Rack. A 370-gal fuel tank was mounted on the outboard pylon. The flight conditions simulated were Mach numbers from 0.29 to 0.78 at an altitude of 5000 ft. For all test conditions, the parent aircraft was in unaccelerated level flight. Also, static stability, axial-force, and trajectory data were obtained for the empty launcher with and without flow through the empty launcher tubes.</p>			

14	KEY WORDS	LINK A		LINK B		LINK C	
		ROLE	WT	ROLE	WT	ROLE	WT
	separation characteristics trajectories bombs (ordnance) LAU-69/A rocket launcher F-4C aircraft Mach numbers fins (folding tail)						